NATIONAL ADVISORY COMMITTEE FOR AERONAUTICS

TECHNICAL NOTE 3451

ANALYSIS OF FULLY DEVELOPED TURBULENT HEAT TRANSFER AND FLOW IN AN ANNULUS WITH VARIOUS ECCENTRICITIES

By Robert G. Deissler and Maynard F. Taylor

Lewis Flight Propulsion Laboratory
Cleveland, Ohio

Washington
May 1955

NATIONAL ADVISORY COMMITTEE FOR AERONAUTICS

TECHNICAL NOTE 3451

ANALYSIS OF FULLY DEVELOPED TURBULENT HEAT TRANSFER AND FLOW IN AN ANNULUS WITH VARIOUS ECCENTRICITIES

By Robert G. Deissler and Maynard F. Taylor

SUMMARY

A previous analysis for turbulent heat transfer and flow in tubes was generalized and applied to an annulus with various eccentricities. Expressions for eddy diffusivity which were verified for flow and heat transfer in tubes were assumed to apply in general along lines normal to a wall. Velocity distributions, wall shear-stress distributions, and friction factors, as well as wall heat-transfer distributions, wall temperature distributions, and average heat-transfer coefficients, were calculated for an annulus having a radius ratio of 3.5 at various eccentricities.

CR-1

INTRODUCTION

Most of the existing analyses for turbulent flow and heat transfer in passages have been confined to circular tubes or parallel plates (refs. 1 to 5). These passages have been analyzed extensively because of their importance in technical applications and because their simplicity makes them amenable to analysis.

In recent years the problems associated with the use of odd-shaped passages in heat exchangers have become important. In reference 6, temperature distributions for rectangular and triangular ducts were calculated by using experimental velocity distributions and average heat-transfer coefficients. No attempt was made to calculate the velocity distributions or heat-transfer coefficients. Some work on the calculation of the velocity and shear-stress distributions in corners is reported in reference 7.

As a part of a general investigation of heat transfer and flow in passages of various shapes being conducted at the NACA Lewis laboratory, the eccentric annulus was analyzed. The methods used in references 4 and 5 for calculating the heat transfer and friction in tubes were extended and applied to annuli having various eccentricities. The methods used herein should be general enough to be applied to passages having various other cross sections.

BASIC EQUATIONS AND ASSUMPTIONS

The differential equations for shear stress and heat transfer can be written in the following form:

$$\tau = (\mu + \rho\epsilon)\frac{du}{dy} \tag{1}$$

$$q = -(k + \rho g c_p \epsilon_h)\frac{dt}{dy} \tag{2}$$

where ϵ and ϵ_h are the eddy diffusivities for momentum and heat transfer, respectively, the values for which are dependent upon the amount and kind of turbulent mixing at a point. In these equations y is taken as the perpendicular distance from the wall. Equations (1) and (2) can be considered as definitions of ϵ and ϵ_h. They can be written in dimensionless form as

$$\frac{\tau}{\tau_0} = \left(\frac{\mu}{\mu_0} + \frac{\rho}{\rho_0}\frac{\epsilon}{\mu_0/\rho_0}\right)\frac{du^+}{dy^+} \tag{3}$$

$$\frac{q}{q_0} = \left(\frac{k}{k_0}\frac{1}{Pr_0} + \frac{\rho}{\rho_0}\frac{c_p}{c_{p_0}}\alpha\frac{\epsilon}{\mu_0/\rho_0}\right)\frac{dt^+}{dy^+} \tag{4}$$

where the subscript 0 refers to values at a wall. All symbols are defined in appendix B.

Expressions for eddy diffusivity. - In order to use equations (3) and (4), the eddy diffusivity ϵ must be evaluated for each portion of the flow. It is assumed, as in references 4 and 5, that in the region at a distance from the wall the mechanism for turbulent transfer is dependent only on the velocities in the vicinity of the point measured relative to the velocity at the point or on the space derivatives of the velocity. In the region close to the wall the turbulence is assumed dependent on quantities measured relative to the wall, that is, u and y.[1] Dimensional analysis then gives, for the region close to the wall ($y^+ < 26$),

$$\epsilon = n^2 u y \tag{5}$$

where the constant n has the experimentally determined value 0.109 (ref. 4).

[1]It was found in reference 8 that in the region very close to the wall ϵ appears to be a function also of kinematic viscosity, but the effect of that factor becomes important only at Prandtl numbers appreciably greater than 1.0.

In the region at a distance from the wall ($y^+ > 26$), ϵ is assumed to be dependent on the relative velocities in the neighborhood of the point. From a Taylor's series expansion for u as a function of y and z,

$$\epsilon = F\left(\frac{\partial u}{\partial y}, \frac{\partial^2 u}{\partial y^2}, \ldots, \frac{\partial u}{\partial z}, \frac{\partial^2 u}{\partial z^2}, \frac{\partial^2 u}{\partial z \partial y} \ldots\right)$$

where y and z are measured in normal directions in the cross section of the passage. In the case of flow in a tube or between parallel plates, the derivatives in the z-direction are zero because the velocity-gradient lines are straight lines normal to the wall. (A velocity-gradient line is a line which at each point is normal to a constant-velocity line.) In an eccentric annulus the velocity-gradient lines near the wall also are normal to the surface, but they are usually curved in the center portion of the passage. Inasmuch as the greatest changes of velocity with respect to distance take place in layers near the wall, the effect of the derivatives with respect to z will be neglected. It seems reasonable to expect that near the center of the flow passage the effect of the derivatives with respect to z would be to increase the turbulence and flatten the profile in that region. However, the normal turbulent profile (derivatives with respect to z absent) is already very flat in that region, so that the increased turbulence should not produce significant changes in the values of the velocities. Therefore, the expression for ϵ for $y^+ > 26$, obtained by using dimensional analysis, and with only the first two derivatives with respect to y considered, is

$$\epsilon = \kappa^2 \frac{(du/dy)^3}{(d^2u/dy^2)^2} \tag{6}$$

where κ has the experimental value 0.36 (ref. 4). This is von Kármán's expression (ref. 1).

Further assumptions. - In order to integrate equations (3) and (4), the following assumptions are made in addition to those concerning the eddy diffusivity (eqs. (5) and (6)):

(1) The fluid properties can be considered constant and the Prandtl number close to 1.0 (0.73). The heat-transfer results are therefore applicable to gases with moderate temperature differences. The analysis could be carried out for variable properties, but the complexity would be increased.

(2) The eddy diffusivities for momentum ϵ and heat transfer ϵ_h are equal, or $\alpha = 1$. Previous analyses for flow in tubes based on this assumption yielded heat-transfer coefficients that agree with experiment (refs. 2 and 5). At low Reynolds or Peclet numbers (Pe = Re Pr), α

appears to be a function of Peclet number (ref. 9), but for Reynolds numbers above 15,000, as in the present analysis, α is nearly constant for gases.

(3) Along the lines normal to the wall, the variations of the shear stress τ and heat transfer per unit area q have a negligible effect on the velocity and temperature distributions. It is shown in figure 11 of reference 5 that the assumption of a linear variation of shear stress and heat transfer across a tube (τ or $q = 0$ at tube center) gives very nearly the same velocity and temperature profiles as those obtained by assuming uniform shear stress and heat transfer across the tube.

(4) The molecular shear-stress and heat-transfer terms in equations (3) and (4) can be neglected in the region at a distance from the wall ($y^+ > 26$)(ref. 5, fig. 12).

Generalized velocity and temperature distributions. - Equations (3) and (4) have been integrated using the foregoing assumptions in references 4 and 5, where the equations are also verified experimentally for flow and heat transfer in tubes. The results are reproduced in figures 1 and 2. These curves give the relations between u^+, y^+, and t^+ which will be used in the following calculations for eccentric annuli.

CALCULATION OF VELOCITY DISTRIBUTIONS FOR ECCENTRIC ANNULI

For applying the relation between u^+ and y^+ in figure 1 to the calculation of velocity distributions in an eccentric annulus, an iterative procedure must be used, inasmuch as the lines of velocity gradient (lines normal to constant-velocity lines) are unknown at the outset. An eccentric annulus, with several assumed velocity-gradient lines, is shown in sketch (a).

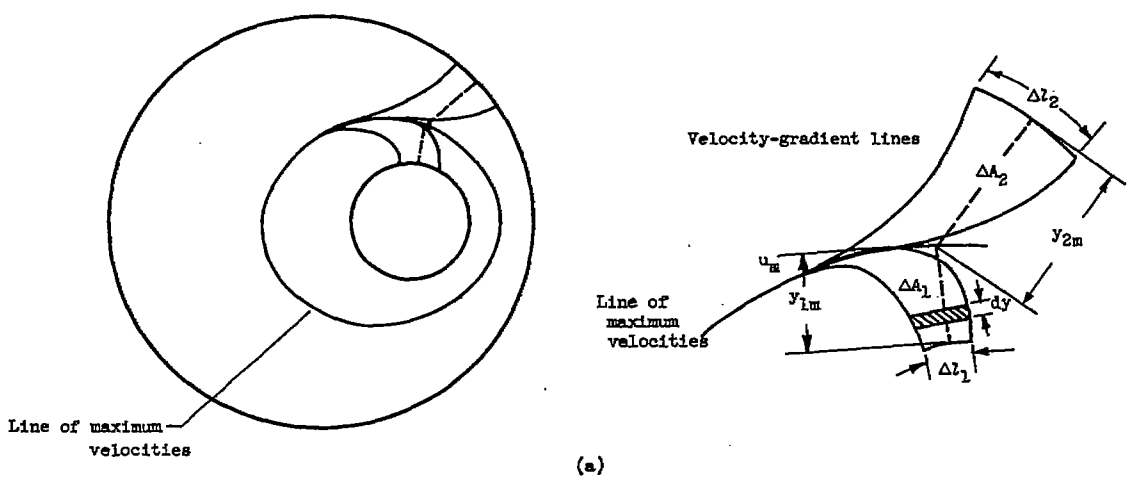

(a)

By using these assumed velocity-gradient lines, lines of constant velocity can be calculated, as will be shown. A new and more accurate set of velocity-gradient lines can then be drawn, inasmuch as they must be normal to the constant-velocity lines. With a little practice, the velocity-gradient lines can be estimated quite accurately the first time so that it is not usually necessary to go through the procedures more than once or twice.

Calculation of line of maximum velocities. - After the velocity-gradient lines have been estimated, the next step is to calculate the line of maximum velocities shown on sketch (a). The velocities on either side of this line are lower than the velocities on the line. Two adjacent velocity-gradient lines are also shown in the sketch. The lengths Δl_1 and Δl_2 are on the inner and outer cylinders, respectively, and the line dividing ΔA_1 and ΔA_2 is the line of maximum velocities. The locations of Δl_1 and Δl_2 must be chosen so that straight lines drawn normal to them at their midpoints (shown dashed in the sketch) meet at the line of maximum velocities. It will be necessary to match the velocities at that point as calculated from the relation between u^+ and y^+ along the normals from Δl_1 and Δl_2. In order to write force balances on the elements ΔA_1 and ΔA_2, the shear forces acting on Δl_1 and Δl_2 and the pressure forces acting on the faces of the elements must be considered. There are no shear forces acting on the velocity-gradient lines, because the normal velocity derivatives are zero along those lines. Writing force balances on ΔA_1 and ΔA_2 results in

$$\tau_1 = - \frac{\Delta A_1}{\Delta l_1} \left(\frac{dp}{dx} \right) \tag{7}$$

$$\tau_2 = - \frac{\Delta A_2}{\Delta l_2} \left(\frac{dp}{dx} \right) \tag{8}$$

where the pressure gradient dp/dx is uniform over the annulus because the flow is fully developed. Dividing equation (8) by equation (7) gives

$$\frac{\tau_2}{\tau_1} = \frac{\Delta l_1}{\Delta l_2} \frac{\Delta A_2}{\Delta A_1} \tag{9}$$

From the curve of u^+ against y^+ (fig. 1),

$$u^+ = F(y^+)$$

Applying this equation to ΔA_1 and ΔA_2 gives

$$\frac{u_1}{\sqrt{\tau_1/\rho}} = F\left(\frac{\sqrt{\tau_1/\rho}}{\mu/\rho}\, y_1\right) \tag{10}$$

and

$$\frac{u_2}{\sqrt{\tau_2/\rho}} = F\left(\frac{\sqrt{\tau_2/\rho}}{\mu/\rho}\, y_2\right) \tag{11}$$

When these equations are evaluated at $u_1 = u_2 = u_m$, and equation (10) is divided by equation (11), there results

$$\sqrt{\frac{\tau_2}{\tau_1}} = \frac{F\left(\frac{\sqrt{\tau_1/\rho}}{\mu/\rho}\, y_{1m}\right)}{F\left(\frac{\sqrt{\tau_2/\rho}}{\mu/\rho}\, y_{2m}\right)} \tag{12}$$

Elimination of τ_1 and τ_2 from equation (12) by use of equations (7) to (9) and conversion to dimensionless form give

$$\frac{\sqrt{\frac{\Delta A_2/\Delta l_2}{r_1}}}{\sqrt{\frac{\Delta A_1/\Delta l_1}{r_1}}} = \frac{F\left(\sqrt{\frac{\Delta A_1/\Delta l_1}{r_1}}\, r_1^{++}\, \frac{y_{1m}}{r_1}\right)}{F\left(\sqrt{\frac{\Delta A_2/\Delta l_2}{r_1}}\, r_1^{++}\, \frac{y_{2m}}{r_1}\right)} = \frac{F\left(y_{1m}^{+}\right)}{F\left(y_{2m}^{+}\right)} = \frac{u_{1m}^{+}}{u_{2m}^{+}} \tag{13}$$

where r_1^{++}, defined by $r_1^{++} \equiv \sqrt{\frac{-r_1\, dp/dx}{\rho}}\, r_1$, is a type of Reynolds number which is assigned an arbitrary value. The quantity y_{1m}/r_1, that is, a point on the line of maximum velocities, can be calculated from equation (13) by trial. Referring to sketch (a), the value for y_{1m}/r_1 is first assumed. Values for $\Delta A_2/(\Delta l_2 r_1)$, $\Delta A_1/(\Delta l_1 r_1)$, and y_{2m}/r_1 can then be calculated by measuring the areas and lengths in the sketch. For a given value of r_1^{++}, then, y_{1m}^{+} and y_{2m}^{+} (terms in parentheses, eq. (13)) can be calculated and u_{1m}^{+}/u_{2m}^{+} obtained from the plot of the relation between u^{+} and y^{+} (fig. 1). If this value of u_{1m}^{+}/u_{2m}^{+} does not agree with the term on the extreme left side of equation (13), another value for y_{1m}/r_1 must be tried. In this way the value for y_{1m}/r_1, and thus a point on the line of maximum velocities, can be found.

Calculation of lines of constant velocity. - For calculating velocities at various points in the annulus, it is convenient to define the following velocity parameter:

$$u_1^{++} \equiv \frac{u_1}{\sqrt{\frac{-r_1 \, dp/dx}{\rho}}} \qquad u_2^{++} \equiv \frac{u_2}{\sqrt{\frac{-r_1 \, dp/dx}{\rho}}} \tag{14}$$

This parameter is used in place of u^+, because the shear stress in the definition of u^+ varies with position. Equation (14) can be written in terms of quantities already known as

$$u_1^{++} = \frac{u_1^+ \, y_{1m}^+}{r_1^{++} \frac{y_{1m}}{r_1}} \tag{15}$$

where

$$u_1^+ = F(y_1^+) = F\left(\frac{y_1}{y_{1m}} \, y_{1m}^+\right) \tag{16}$$

where the function F is obtained from the relation between u^+ and y^+ in figure 1. Equations (15) and (16) apply to points lying between the inner cylinder and the line of maximum velocities. For points between the outer cylinder and the line of maximum velocities, these equations are replaced by

$$u_2^{++} = \frac{u_2^+ \, y_{2m}^+}{r_1^{++} \frac{y_{2m}}{r_1}} \tag{17}$$

where

$$u_2^+ = F\left(\frac{y_2}{y_{2m}} \, y_{2m}^+\right) \tag{18}$$

The quantities y_{1m}^+, y_{2m}^+, y_{1m}/r_1, and y_{2m}/r_1 are already known from equation (13). The relation between u_1^{++} and y_1/y_{1m} or u_2^{++} and y_2/y_{2m} for a given r_1^{++} can therefore be calculated along a given line normal to the inner or outer cylinder.

By carrying out the calculation for various lines normal to the inner or outer cylinder, lines of constant velocity (constant u^{++}) can be obtained. As mentioned previously, new and more accurate velocity-gradient lines are next drawn so as to intersect the constant-velocity lines at right angles. The calculation is then repeated using the new velocity-gradient lines.

Calculated velocity distributions. - Several velocity distributions for eccentric annuli, as calculated by the method described, are shown in figure 3. The calculations were carried out for an annulus having a diameter ratio of $3\frac{1}{2}$ for various eccentricities. The shape of the constant-velocity lines indicates, as would be expected, that the greatest velocities occur on the side where the separation of the cylinders is greatest, and that the velocities on the side where the separation is least are much smaller and go to zero when the cylinders touch. Although the velocity distributions are plotted for an r_1^{++} of 200, the constant-velocity lines for an r_1^{++} of 4000 have practically the same shape. The values of $u/u_{b,av}$ are slightly different for the two values of r_1^{++}, but the difference is not large.

In all cases the line of maximum velocities lies closer to the inner than to the outer cylinder, that is, it lies closer to the surface having the smaller area.

In most cases the calculated constant-velocity lines shown in figure 3 are very nearly normal to the velocity-gradient lines, as required. However, in some cases, especially for the large eccentricities, difficulty was experienced in obtaining normal lines in some regions. Whether this lack of normalcy is due to the fact that the iterations were not carried far enough or to the approximate nature of some of the assumptions made in the analysis has not been established. However, the difficulty occurs only in regions in which the velocity gradients are very small, so that the error in the computed values of velocity should be small.

FRICTION FACTOR AND REYNOLDS NUMBER

Once the velocity distributions for the annuli have been obtained, friction factors and Reynolds numbers can be calculated by integrating the distributions to obtain bulk or average velocities. The bulk velocity between two adjacent straight lines normal to the wall (dashed lines in sketch (a)) is first obtained. This bulk velocity varies with position on the inner cylinder and is given by

$$u_b \equiv \frac{\int_0^{\Delta A} u \, dA}{\Delta A} \tag{19}$$

where ΔA is the total area between two adjacent straight lines normal to the wall (on both sides of the line of maximum velocities). Equation (19) can be written in dimensionless form as

$$u_b^{++} = \frac{\int_0^{\Delta A} u^{++} \, dA}{\Delta A} \tag{20}$$

The average bulk velocity for the whole annulus can be written as

$$u_{b,av}^{++} = \frac{1}{A} \int_0^{A} u_b^{++} \, dA \tag{21}$$

where A is the total area of the annulus. The variation of $u_b^{++}/u_{b,av}^{++} = u_b/u_{b,av}$ with angle and eccentricity is shown in figure 4.

For later comparison with heat transfer, the local friction factor based on the shear stress on the inner cylinder and the average bulk velocity is introduced and is defined as

$$f_{\tau_1} \equiv \frac{2\tau_1}{\rho u_{b,av}^2} \tag{22}$$

or, in terms of known dimensionless quantities, can be written as

$$f_{\tau_1} = 2\left[\frac{y_{1m}^+}{u_{b,av}^{++} \, r_1^{++}(y_{1m}/r_1)}\right]^2 \tag{23}$$

The average friction factor based on the shear stress is, then,

$$f_{\tau_{1,av}} = \frac{1}{\pi} \int_0^{\pi} f_\tau \, d\theta \tag{24}$$

where θ is the angle at the center of the inner cylinder measured from the line of least separation of the two cylinders. Division of equation (22) by equation (24) gives

$$\frac{f\tau_l}{f_{\tau_{l,av}}} = \frac{\tau_l}{\tau_{l,av}} \tag{25}$$

The ratio $\tau_l/\tau_{l,av}$ could have been obtained directly from equation (7) and a corresponding equation for the whole annulus as

$$\frac{\tau_l}{\tau_{l,av}} = \frac{\Delta A_l}{A_l}\frac{l_l}{\Delta l_l}$$

Curves for $\tau_l/\tau_{l,av}$ or $f_{\tau_l}/f_{\tau_{l,av}}$ against angle θ are presented in figure 5. The curves indicate a decrease in shear stress on the side of the inner cylinder which is closest to the outer cylinder, and a shear stress of zero where the cylinders touch ($e = 1.0$). As in the case of the velocity distributions (fig. 4) the value of r_l^{++} or Reynolds number has a negligible effect on the shape of the curves. The values for the Reynolds numbers were calculated from

$$Re = \frac{u_{b,av}^{++}\, r_l^{++}}{r_l/D_e} \tag{26}$$

which follows directly from the definition of Reynolds number. The equivalent diameter D_e is equal to the difference between the diameters of the outer and inner cylinders. A cross plot of figure 5 for the point of least separation ($\tau_l/\tau_{l,av}$ against eccentricity) is given in figure 6.

The fact that the shear stress should decrease in the region of least separation of the cylinders can be seen directly from equation (7), which indicates that the shear stress is proportional to $\Delta A_l/\Delta l_l$. But $\Delta A_l \sim \Delta l_l y_{lm}$, and, hence, the shear stress is approximately proportional to y_{lm}, which decreases as the distance between cylinders decreases.

The friction factor for the annulus based on the pressure gradient is defined by

$$f \equiv -\frac{D_e\, dp/dx}{2\rho u_{b,av}^2} \tag{27}$$

or, in terms of known dimensionless groups,

$$f = \frac{1}{2(r_l/D_e)u_{b,av}^{++2}} \tag{28}$$

Friction factors based on the pressure gradient are presented in figure 7 as a function of Reynolds number and eccentricity. Comparison of these friction factors with those for a circular tube indicates fair agreement for the case when the cylinders are concentric. The values of the friction factor decrease as the eccentricity is increased; and, for the case where the cylinders touch, the friction factors are approximately 70 percent of those for concentric cylinders.

HEAT-TRANSFER DISTRIBUTION ON INNER CYLINDER WITH OUTER CYLINDER INSULATED

With the information on the velocity distributions obtained in the preceding section and with certain assumptions, the fully developed heat-transfer distributions on the inner cylinder when the inner cylinder is heated (or cooled) and the outer cylinder is insulated can be calculated. Peripheral wall temperature distributions will be calculated from these heat-transfer distributions in the next section.

The heat added between two straight lines normal to the wall per unit length of annulus is $q_l \Delta l_l$ (see sketch (a)'). It is assumed herein that all this heat is used in heating the fluid element between the straight lines (on both sides of the line of maximum velocities). That is, the net heat transfer across the sides of the element is assumed small compared with that transferred through the wall. This assumption is valid when the variation of wall temperature is not too great and the Prandtl number is close to or greater than unity.

Making a heat balance on the element of fluid between two straight lines and using the foregoing assumption result in[2]

$$q_l \Delta l_l = \rho g u_b c_p \left(\frac{dt_b}{dx}\right) \Delta A \tag{29}$$

For the whole annulus

$$q_{l,av} l_l = \rho g u_{b,av} c_p \left(\frac{dt_{b,av}}{dx}\right) A_O \tag{30}$$

---

[2]As an alternative assumption, an element bounded by velocity-gradient lines rather than by straight lines was used. No net heat transfer across the velocity-gradient lines was assumed. This assumption was found to give essentially the same distribution of q_l as did the assumption used in the text.

It is shown in appendix A that, for the fully developed case, $dt_b/dx = dt_{b,av}/dx$ when the heat transfer per unit area at a given angle θ does not vary with x. Division of equation (29) by equation (30) and conversion to dimensionless form give

$$\frac{q_1}{q_{1,av}} = \frac{u_b^{++}}{u_{b,av}^{++}} \frac{\Delta A}{A_0} \frac{l_1}{\Delta l_1} \tag{31}$$

It can easily be shown that equation (31) also gives the ratio of local Nusselt number to average Nusselt number for the case of uniform circumferential wall temperature, since, for that case,

$$h = \frac{q_1}{t_1 - t_{b,av}} = \frac{q_1}{t_{1,av} - t_{b,av}} \tag{32}$$

and

$$h_{av} = \frac{q_{1,av}}{t_{1,av} - t_{b,av}} \tag{33}$$

or

$$\frac{h}{h_{av}} = \frac{Nu}{Nu_{av}} = \frac{q_1}{q_{1,av}} \tag{34}$$

Equation (34) is strictly true only for the case of uniform circumferential wall temperature, because for any other temperature distribution the temperature differences in equations (32) and (33) will not cancel.

Values of $q_1/q_{1,av}$ (h/h_{av} for uniform circumferential wall temperature) are shown as a function of angle and of eccentricity in figure 8. As was the case with the shear stress (fig. 5), the heat transfer is low on the side of the cylinder where the separation of the cylinder is least and approaches zero when the cylinders touch. However, comparison of figures 5 and 8 indicates that the heat transfer approaches zero much more rapidly than does the shear stress. The same trends are indicated by comparison of figures 6 and 9, where $\tau_1/\tau_{1,av}$ and $q_1/q_{1,av}$ are plotted against eccentricity for the point of least separation of the cylinders. Comparison of these figures indicates, therefore, that the assumption of similarity of the shear-stress and heat-transfer-coefficient distributions, which is usually made in analyses for odd-shaped passages, might give heat-transfer coefficients in the vicinity of a corner that are too high. This was pointed out in reference 10. Experimental wall temperature distributions in reference 11 indicated that in some cases the predicted coefficients were too high.

The reason that the heat transfer decreases more rapidly than the shear stress as the line of least separation of the cylinders is approached can easily be seen by comparison of equations (7) and (29). Both equations contain $\Delta A/\Delta l_1$ or $\Delta A_1/\Delta l_1$, which causes the heat transfer or shear stress to decrease near the line of least separation. However, the heat-transfer equation (eq. (29)) contains, in addition, the local bulk velocity u_b, which also decreases; therefore, the heat transfer decreases more rapidly than the shear stress as the line of least separation is approached.

WALL TEMPERATURE DISTRIBUTION

The inner cylinder of the annulus is assumed, in this section, to be the outside surface of a thin-walled tube. Heat is transferred uniformly to the inside surface of the tube. Because of tangential conduction around the tube, the heat transfer through the outer surface to the fluid will not be uniform and will have the distribution obtained in the preceding section. Since the tube is thin-walled and there are no heat sources in the tube, the heat transfer per unit area through the inner surface is equal to $q_{1,av}$, the average heat transfer per unit area through the outer surface to the fluid. As in the previous section, the outer cylinder of the annulus is insulated.

In order to obtain the temperature distribution around the tube, a heat balance is first made on an element of tube of circumferential length dl. This heat balance gives

$$q_{1,av} - q_1 = b \frac{dq_t}{dl_1} \tag{35}$$

where b is the thickness of the tube and q_t is the tangential heat conduction for unit area. Equation (35) can be written in integral form as

$$\int_0^{l_1/r_1} \left(1 - \frac{q_1}{q_{1,av}}\right) d\left(\frac{l_1}{r_1}\right) = \frac{b}{q_{1,av} r_1} \int_0^{q_t} dq_t = \frac{b}{q_{1,av} r_1} q_t \tag{36}$$

where $l_1/r_1 = \theta$ and q_t is zero for $l_1 = 0$, the point of least separation of the cylinders, because the wall temperature distribution is symmetric about that point (the temperature gradient is zero). But

$$q_t = - k_t \frac{dt_1}{dl_1} \tag{37}$$

Substituting equation (37) in equation (36) and integrating again result in

$$\int_0^\theta \left[\int_0^\theta \left(1 - \frac{q_1}{q_{1,av}} \right) d\theta \right] d\theta = \frac{bk_t(t_{1,max} - t_1)}{q_{1,av} r_1^2} \tag{38}$$

where $t_{1,max}$ is the wall temperature at the point of least separation of the cylinders. By using the values of $q_1/q_{1,av}$ obtained in the preceding section, the difference between the maximum wall temperature and the wall temperature at any angle for a given heat flux can be calculated from equation (38). A dimensionless parameter containing the difference between the maximum and the average wall temperatures can be obtained by integrating equation (38), that is

$$\frac{bk_t(t_{1,max} - t_{1,av})}{q_{1,av} r_1^2} = \frac{1}{\pi} \int_0^\pi \frac{bk_t(t_{1,max} - t_1)}{q_{1,av} r_1^2} d\theta \tag{39}$$

The relation for $bk_t(t_1 - t_{1,av})/(q_{1,av} r_1^2)$ can be obtained by subtracting equation (38) from equation (39).

The results for the wall temperature distributions are presented in figure 10, where $bk_t(t_1 - t_{1,av})/(q_{1,av} r_1^2)$ is plotted against angle for various eccentricities, and in figure 11, where $bk_t(t_{1,max} - t_{1,av})/(q_{1,av} r_1^2)$ is plotted against eccentricity. It is of interest that $t_{1,max} - t_{1,av}$, which is the quantity of greatest practical interest, can be obtained from a single curve. That is, for a given annulus, only two dimensionless parameters are involved. For a given eccentricity, $t_{1,max} - t_{1,av}$ is directly proportional to the uniform heat flux through the inside surface of the tube.

Wall temperature distributions for various other cases, such as the case where the tube wall is not thin or where internal heat sources are present in the tube wall, can also be readily calculated by using the heat-transfer distributions in figure 8. In order to use these distributions it is, of course, necessary that the outer cylinder be insulated.

NUSSELT NUMBER

For obtaining all the results thus far (wall heat-transfer distributions, wall temperature distributions, etc.), it was not necessary to use the generalized temperature distribution in figure 2. However, it is necessary to use that distribution for obtaining the difference between wall and bulk temperatures which corresponds to a given heat flow, that is, for obtaining the heat-transfer coefficient.

Average heat-transfer coefficient. - The average heat-transfer coefficient for the inner wall of the annulus is defined by

$$h_{av} \equiv \frac{q_{1,av}}{t_{1,av} - t_{b,av}} \tag{40}$$

where

$$t_{1,av} = \frac{1}{\pi} \int_0^{\pi} t_1 \, d\theta \tag{41}$$

$$t_b = \frac{\int_0^{\Delta A} tu \, dA}{u_b \Delta A} \tag{42}$$

and

$$t_{b,av} = \frac{\int_0^{A_0} t_b u_b \, dA}{u_{b,av} A_0} \tag{43}$$

The average Nusselt number corresponding to the average heat-transfer coefficient (eq. (40)) can be calculated from the following equation, which can be verified by substituting the definitions of the various quantities:

$$\frac{1}{Nu_{av}} = \frac{r_1/D_e}{r_1^{++}Pr} \int_0^1 t_b^{++}(u_b/u_{b,av})d(A/A_0) -$$

$$\frac{r_1}{D_e}\frac{kr_1}{k_t b} \int_0^1 \frac{k_t b(t_1 - t_{1,av})}{q_{1,av} r_1^2} \left(\frac{u_b}{u_{b,av}}\right) d\left(\frac{A}{A_0}\right) \qquad (44)$$

where

$$t_b^{++} = \int_0^1 t_1^{++} \frac{u^{++}}{u_b^{++}} d\left(\frac{A}{\Delta A}\right) \qquad (45)$$

and

$$t_1^{++} = \frac{t_1^{+} r_1^{++} y_{1m}/r_1}{y_{1m}^{+}} \qquad (46)$$

Equation (46) applies to the region between the inner cylinder and the line of maximum velocities. For the region between the outer cylinder and the line of maximum velocities, y_{1m} and y_{1m}^{+} are replaced by y_{2m} and y_{2m}^{+}, respectively. As in the case of velocity distributions, the values of y^{+} are measured along normals to the inner or outer cylinder which extend to the line of maximum velocities. The values of t^{+} are obtained from figure 2. In the present case, where the outer wall is insulated, figure 2 indicates that the temperature is uniform along the normals drawn from the outer cylinder to the line of maximum velocities. Since $q_2 = 0$, $t_2 - t$ must also be zero, inasmuch as t^{+} is finite. In the actual case t would vary somewhat along the lines normal to the outer cylinder. However, a constant t is consistent with the assumptions made in the present analysis, and the error produced is small because the actual temperature gradients are small in the region between the outer cylinder and the line of maximum velocities.

Average Nusselt numbers calculated by equation (44) are plotted against eccentricity for a range of Reynolds numbers and for values of the parameter $kr_1/k_t b$ of zero and 0.01 in figure 12. The wall temperature distributions were obtained from figure 10. For the case where the cylinders are concentric, the Nusselt numbers are in good

agreement with those obtained by the conventional Nusselt equation for tubes or the predicted relation for tubes in reference 5. The average Nusselt numbers decrease with increasing eccentricity (fig. 12) as did the friction factors (fig. 6). For the maximum eccentricity the average Nusselt numbers decrease to about one-fifth their values for zero eccentricity. The curves also indicate a substantial effect of wall temperature distribution kr_1/k_tb on the Nusselt numbers. The Nusselt numbers decrease as kr_1/k_tb increases or as tube conductivity or thickness decreases. The effect of peripheral wall temperature distribution on average Nusselt number is not generally considered in analyses

Local heat-transfer coefficient. - The local heat-transfer coefficient at a given angle θ is defined as

$$h \equiv \frac{q_1}{t_1 - t_{b,av}} \tag{47}$$

The local Nusselt number corresponding to h can be calculated from

$$Nu = \frac{q_1/q_{1,av}}{\frac{r_1}{D}\frac{(t_1 - t_{1,av})bk_t}{q_{1,av}r_1^2}\frac{kr_1}{k_tb} + \frac{1}{Nu_{av}}} \tag{48}$$

It can be seen from equation (48) that, for uniform circumferential wall temperature, $Nu/Nu_{av} = h/h_{av} = q_1/q_{1,av}$, as mentioned previously (fig. 8).

Values of $Nu/Nu_{av} = h/h_{av}$ for a value of kr_1/k_tb of 0.01 are plotted as functions of angle θ and of eccentricity in figure 13. These curves are strongly affected by changes in Reynolds number, in contrast to most of the preceding results, because the second term in the denominator of equation (48) varies considerably with Reynolds number, whereas the first term is nearly constant.

It might be mentioned that local heat-transfer coefficients are not essential to give a complete description of the heat transfer in eccentric annuli. Most quantities of interest could be obtained from the plots of wall heat-transfer distribution, wall temperature distribution, and average Nusselt number. The local heat-transfer coefficients are given as a matter of interest, inasmuch as most persons concerned with heat transfer usually consider local heat-transfer coefficients rather than local heat-transfer rates.

SUMMARY OF RESULTS

The following results were obtained from the analytical investigation of fully developed turbulent heat transfer and flow in eccentric annuli:

1. The maximum velocities in the annulus occurred closer to the inner than to the outer cylinder. The location of the line of maximum velocities was essentially independent of Reynolds number.

2. When the cylinders were not concentric, the velocities and shear stresses in the region where the separation of the cylinders was least were lower than the average values and approached zero when the cylinders touched.

3. When the inner cylinder was heated and the cylinders were not concentric, the heat transfer to the fluid in the region where the separation of the cylinders was least was lower than the average value and approached zero when the cylinders touched. For the case where the cylinders touched, the heat transfer approached zero much more rapidly than did the shear stress as the line of contact was approached.

4. The friction factors for the annulus with the cylinders concentric were very slightly higher than those for a circular tube. As the eccentricity increased, the friction factors decreased.

5. When the outside surface of a thin-walled tube was assumed to form the inner cylinder of the annulus and heat was applied uniformly to the inside surface of the tube, the difference between the maximum and average wall temperatures for a given eccentricity was directly proportional to the heat flux.

6. The average Nusselt numbers for the annulus with the cylinders concentric were very slightly higher than those for a tube. As the eccentricity increased, the Nusselt numbers decreased. The average Nusselt number was also found to be a function of peripheral wall temperature distribution.

Lewis Flight Propulsion Laboratory
National Advisory Committee for Aeronautics
Cleveland, Ohio, March 16, 1955

APPENDIX A

CONDITION FOR FULLY DEVELOPED HEAT TRANSFER

For fully developed heat transfer and constant fluid properties,

$$\frac{q_1}{t_1 - t_a} = h_a \tag{A1}$$

where h_a, an arbitrary heat-transfer coefficient, is independent of x. If h_a were not independent of x at a great distance from the entrance (cyclic variations of h_a excluded), the absolute value of h_a would become arbitrarily large as x increased so that for finite temperature differences the absolute value of q_1 would become arbitrarily large. The following equations are special cases of equation (A1):

$$\frac{q_1}{t_1 - t_{b,av}} = h \tag{A2}$$

$$\frac{q_1}{t_1 - t_b} = h_1 \tag{A3}$$

For the case where the wall heat transfer per unit area is independent of x (but not of θ), equations (A2) and (A3) can be differentiated to give the following results:

$$\frac{dt_1}{dx} = \frac{dt_{b,av}}{dx}$$

$$\frac{dt_1}{dx} = \frac{dt_b}{dx}$$

or

$$\frac{dt_b}{dx} = \frac{dt_{b,av}}{dx} \tag{A4}$$

The quantity dt_b/dx is therefore independent of θ when the heat transfer is independent of x.

APPENDIX B

SYMBOLS

The following symbols are used in this report:

A_0	total area between inner cylinder and outer cylinder, sq ft
A_1	total area between inner cylinder and line of maximum velocities, sq ft
A_2	total area between outer cylinder and line of maximum velocities, sq ft
b	wall thickness of inner tube, ft
c_p	specific heat of fluid at constant pressure, Btu/(lb)(°F)
D	diameter, ft
D_e	equivalent diameter of annulus, $D_2 - D_1$, ft
g	conversion factor, 32.2 ft/sec^2
h	local heat-transfer coefficient, $\frac{q_l}{t_l - t_{b,av}}$, $\frac{\text{Btu}}{(\text{sec})(\text{sq ft})(^\circ\text{F})}$
h_{av}	average heat-transfer coefficient, $\frac{q_{l,av}}{t_{l,av} - t_{b,av}}$, $\frac{\text{Btu}}{(\text{sec})(\text{sq ft})(^\circ\text{F})}$
k	thermal conductivity of fluid, Btu/(sec)(sq ft)(°F/ft)
k_t	thermal conductivity of material of inner cylinder, Btu/(sec)(sq ft)(°F/ft)
l	peripheral distance along wall, ft
p	static pressure, lb/sq ft abs

q_1	rate of heat transfer from wall of inner cylinder per unit area, Btu/(sec)(sq ft)
$q_{1,av}$	average rate of heat transfer from wall of inner cylinder per unit area, Btu/(sec)(sq ft)
r	radius, ft
t	temperature of fluid at a point, $^{\circ}F$
t_a	arbitrary temperature
t_b	local bulk temperature of fluid at given angle at cross section of annulus, $^{\circ}F$
t_0	wall temperature, $^{\circ}F$
t_1	local wall temperature of inner cylinder or tube, $^{\circ}F$
$t_{1,max}$	maximum wall temperature of inner cylinder or tube, $^{\circ}F$
u	time-averaged velocity parallel to wall at a point, ft/sec
u_b	local bulk velocity at given angle at cross section of annulus, ft/sec
u_m	velocity at a point on line of maximum velocities, ft/sec
x	axial distance along annulus, ft
y	normal distance from wall, ft
y_{1m}	value of y_1 at $u = u_m$, ft
y_{2m}	value of y_2 at $u = u_m$, ft
ϵ	coefficient of eddy diffusivity for momentum, sq ft/sec
ϵ_h	coefficient of eddy diffusivity for heat, sq ft/sec
θ	angle made with center of inner tube, radians

μ absolute viscosity of fluid, (lb)(sec)/sq ft

ρ mass density, $(lb)(sec^2)/ft^4$

τ shear stress in fluid, lb/sq ft

Dimensionless quantities:

$\frac{bk_t(t_{1,max} - t_{1,av})}{q_{1,av}r_1^2}$ wall-temperature-distribution parameter where angle is zero

$\frac{bk_t(t_1 - t_{1,av})}{q_{1,av}r_1^2}$ wall-temperature-distribution parameter

e eccentricity parameter, distance between centers of cylinders divided by $r_2 - r_1$

f friction factor, $\frac{-D_e \frac{dp}{dx}}{2\rho u_{b,av}^2}$

f_{τ_1} friction factor, $\frac{2\tau_1}{\rho u_{b,av}^2}$

Nu Nusselt number based on local heat transfer, $\frac{hD_e}{k}$

Nu_{av} Nusselt number based on average heat transfer, $\frac{h_{av}D_e}{k}$

n constant, 0.109

Pr Prandtl number, $c_p\mu g/k$

Re Reynolds number, $\frac{\rho u_b D_e}{\mu}$

r_1^{++} inner-tube radius parameter, $\frac{\sqrt{\frac{-r_1 \, dp/dx}{\rho}}}{\mu/\rho} r_1$

t^+ temperature parameter, $\dfrac{(t_0 - t)c_{p_0} g \tau_0}{q_0 \sqrt{\tau_0/\rho_0}}$

t_b^{++} bulk-temperature parameter, $\displaystyle\int_0^1 t_1^{++} \frac{u^{++}}{u_b^{++}} \, d\left(\frac{A}{\Delta A}\right)$

t_1^+ temperature parameter, $\dfrac{(t_1 - t)c_p g \tau_1}{q_1 \sqrt{\tau_1/\rho}}$

t_1^{++} temperature parameter, $\dfrac{(t_1 - t)c_p g \rho \sqrt{\dfrac{-r_1 \frac{dp}{dx}}{\rho}}}{q_1}$

u^+ velocity parameter, $\dfrac{u}{\sqrt{\tau_0/\rho_0}}$

u^{++} velocity parameter, $\dfrac{u}{\sqrt{\dfrac{-r_1 \, dp/dx}{\rho}}}$

u_b^{++} bulk-velocity parameter, $\dfrac{\displaystyle\int_0^{\Delta A} u \, dA}{\Delta A}$

$u_{b,av}^{++}$ bulk-velocity parameter, $\dfrac{1}{A} \displaystyle\int_0^A u_b \, dA$

u_1^+ velocity parameter, $\dfrac{u_1}{\sqrt{\tau_1/\rho}}$

u_2^+ velocity parameter, $\dfrac{u_2}{\sqrt{\tau_2/\rho}}$

u_{lm}^+ u_1^+ evaluated at line of maximum velocities

u_{2m}^+	u_2^+ evaluated at line of maximum velocities
y_1^+	wall-distance parameter, $\frac{\sqrt{\tau_1/\rho}}{\mu/\rho} y_1$
y_2^+	wall-distance parameter, $\frac{\sqrt{\tau_2/\rho}}{\mu/\rho} y_2$
y_{1m}^+	y_1^+ evaluated at line of maximum velocities
y_{2m}^+	y_2^+ evaluated at line of maximum velocities
α	ratio of eddy diffusivity for heat transfer to eddy diffusivity for momentum transfer, ϵ_h/ϵ
$\varkappa$	Kármán constant, 0.36

Subscripts:

a	arbitrary
0	pertaining to a wall
1	pertaining to inner cylinder
2	pertaining to outer cylinder

REFERENCES

1. von Kármán, Th.: Turbulence and Skin Friction. Jour. Aero. Sci., vol. 1, no. 1, Jan. 1934, pp. 1-20.

2. von Kármán, Th.: The Analogy Between Fluid Friction and Heat Transfer. Trans. A.S.M.E., vol. 61, no. 8, Nov. 1939, pp. 705-710.

3. Martinelli, R. C.: Heat Transfer to Molten Metals. Trans. A.S.M.E., vol. 69, no. 8, Nov. 1947, pp. 947-959.

4. Deissler, Robert G.: Analytical and Experimental Investigation of Adiabatic Turbulent Flow in Smooth Tubes. NACA TN 2138, 1950.

5. Deissler, R. G.: Heat Transfer and Fluid Friction for Fully Developed Turbulent Flow of Air and Supercritical Water with Variable Fluid Properties. Trans. A.S.M.E., vol. 76, no. 1, Jan. 1954, pp. 73-85.

6. Eckert, E. R. G., and Low, George M.: Temperature Distribution in Internally Heated Walls of Heat Exchangers Composed of Noncircular Flow Passages. NACA Rep. 1022, 1951. (Supersedes NACA TN 2257.)

7. Elrod, Harold G., Jr.: Turbulent Heat Transfer in Polygonal Flow Sections. NDA-10-7, Nuclear Dev. Associates, Inc. (New York), Sept. 22, 1952. (Purchase Order 267031.)

8. Deissler, Robert G.: Analysis of Turbulent Heat Transfer, Mass Transfer, and Friction in Smooth Tubes at High Prandtl and Schmidt Numbers. NACA TN 3145, 1954.

9. Deissler, Robert G.: Analysis of Fully Developed Turbulent Heat Transfer at Low Peclet Numbers in Smooth Tubes with Application to Liquid Metals. NACA RM E52F05, 1952.

10. Eckert, E. R. G.: Temperature Distribution in the Walls of Heat Exchangers with Noncircular Flow Passages. Heat Transfer and Fluid Mech. Inst., Univ. Calif., 1952, pp. 175-186.

11. Lowdermilk, Warren H., Weiland, Walter F., Jr., and Livingood, John N. B.: Measurement of Heat-Transfer and Friction Coefficients for Flow of Air in Noncircular Ducts at High Surface Temperatures. NACA RM E53J07, 1954.

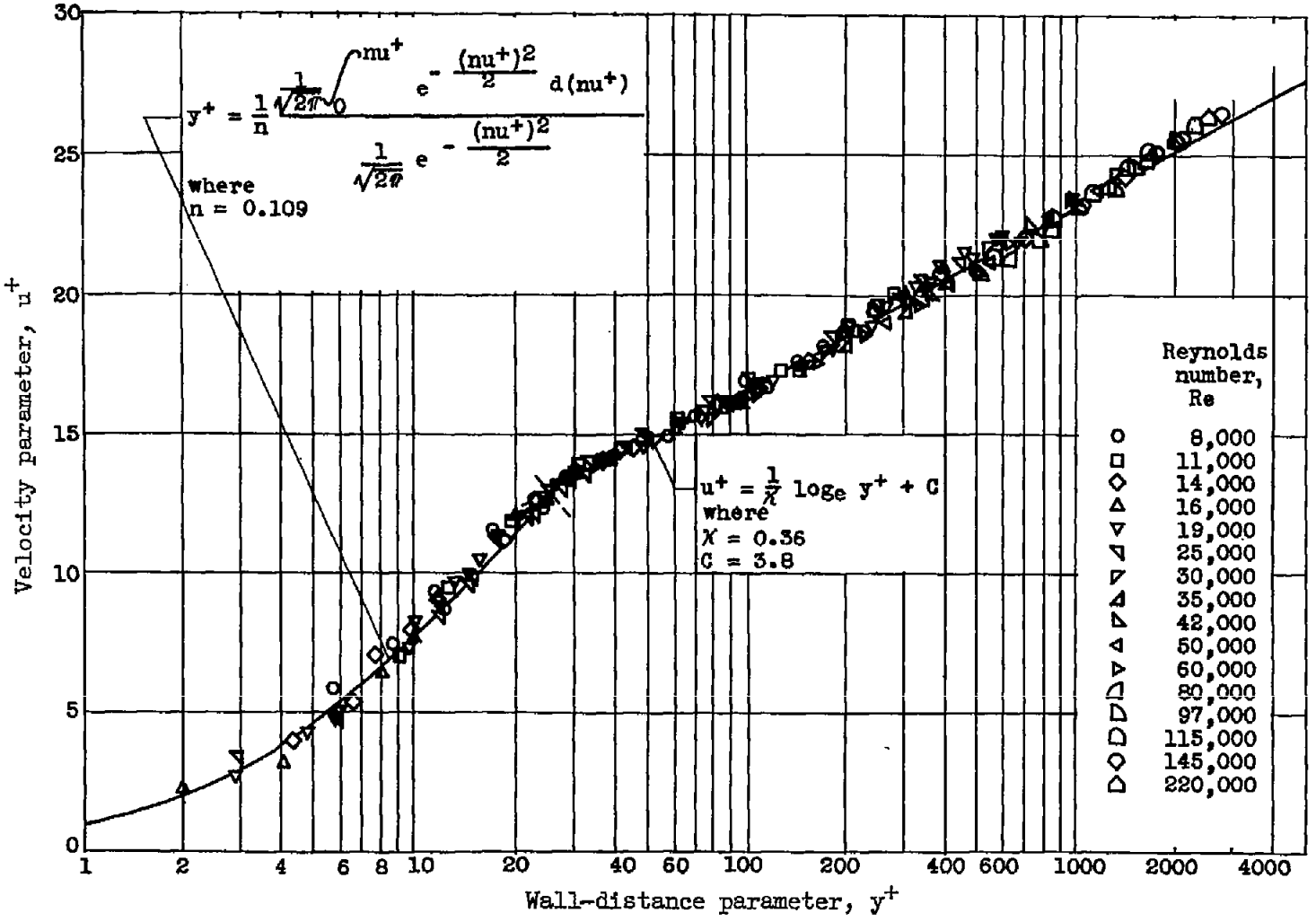

Figure 1. - Generalized velocity distribution for fully developed turbulent flow in smooth tubes (ref. 10).

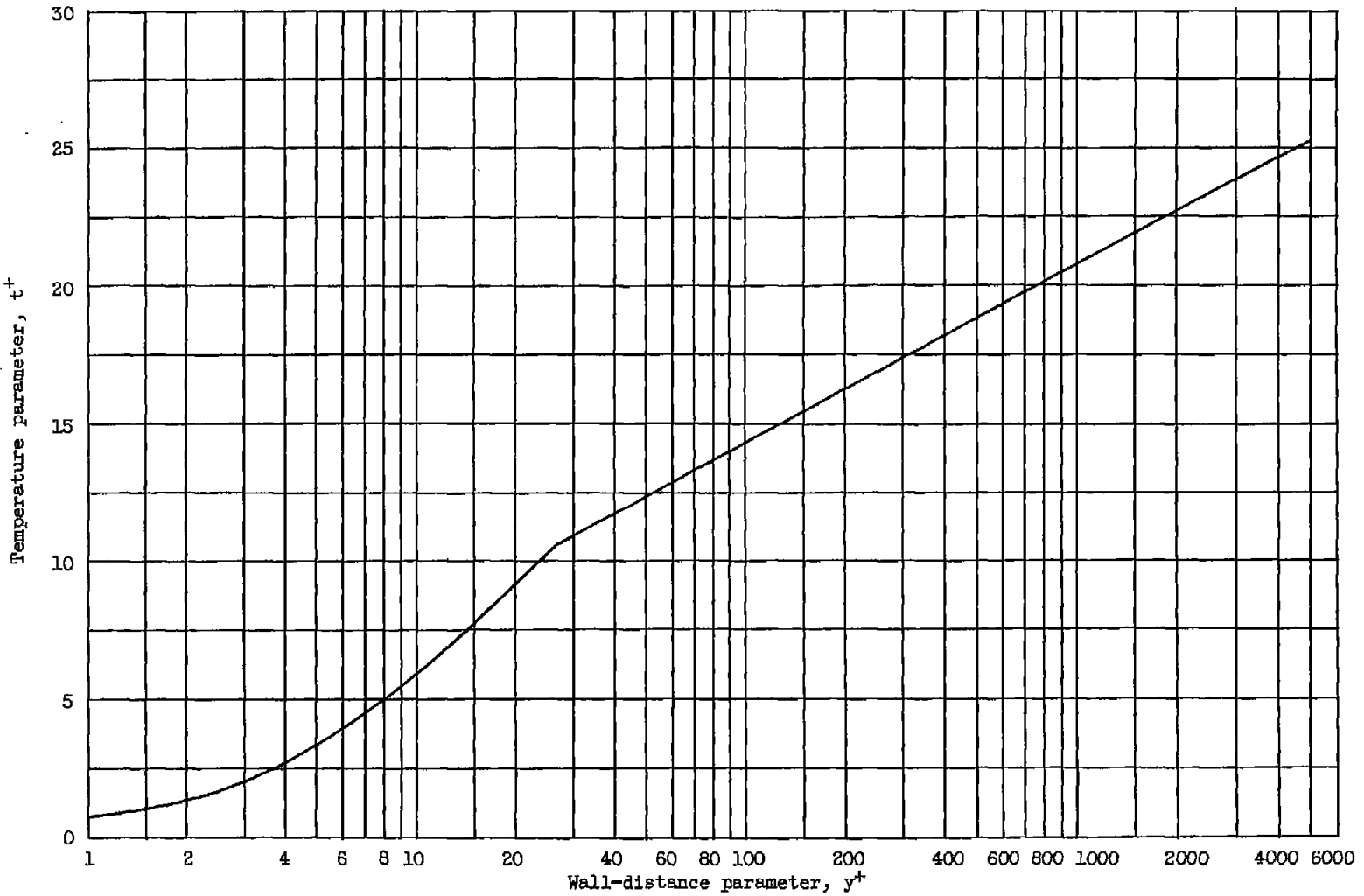

Figure 2. - Predicted generalized temperature distribution for flow of air. Prandtl number, 0.73.

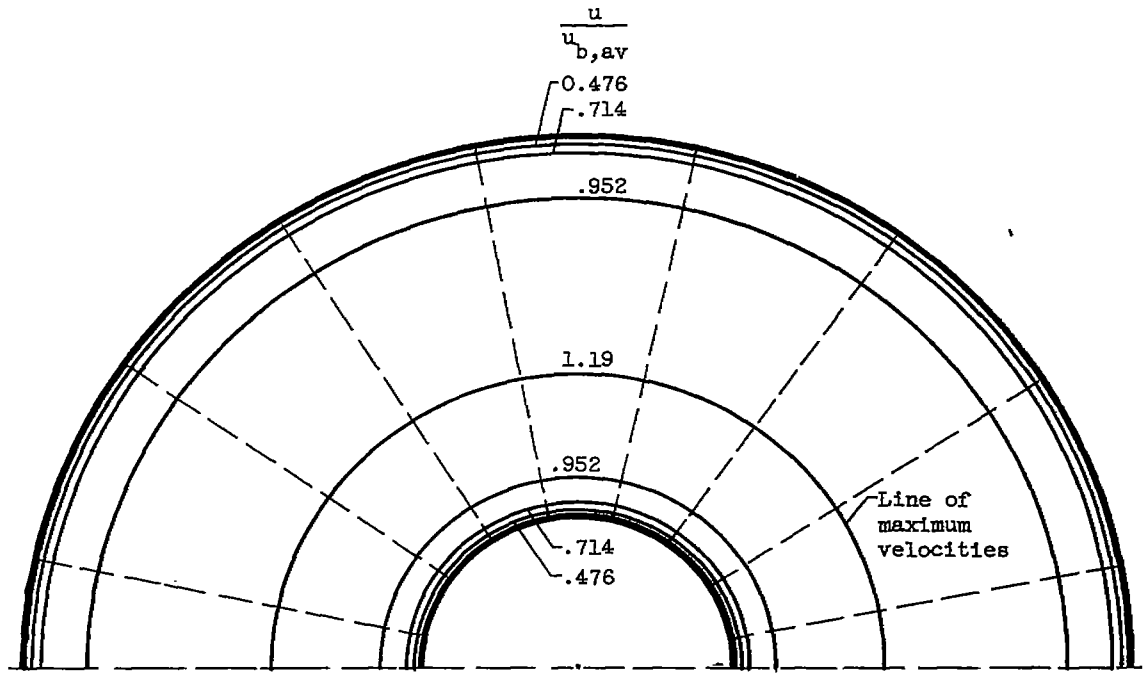

(a) Eccentricity parameter, 0.

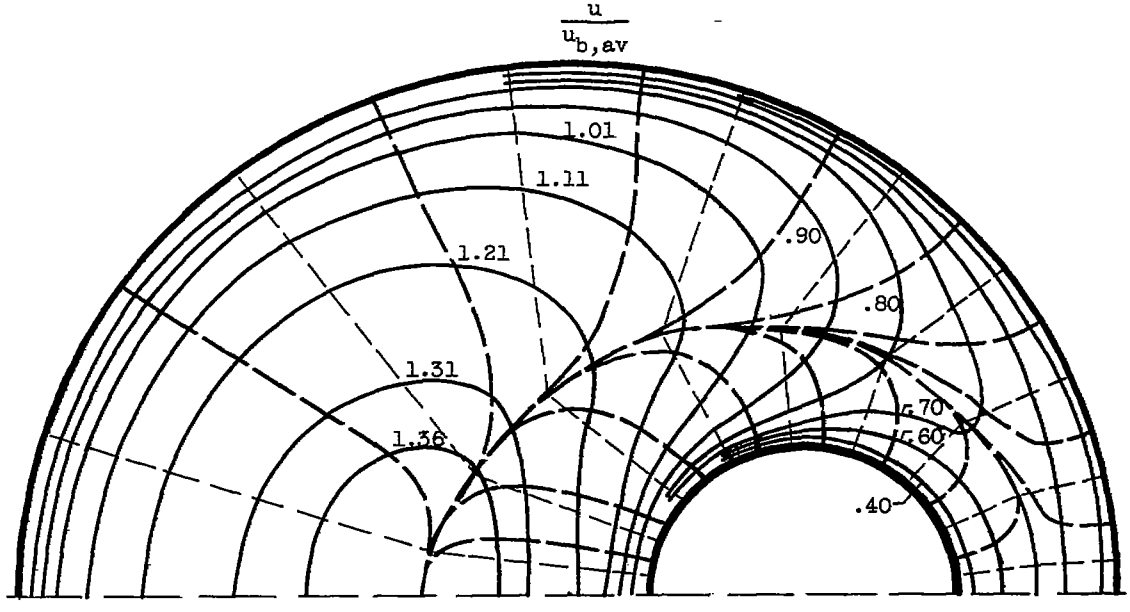

(b) Eccentricity parameter, 0.6.

Figure 3. - Predicted velocity distributions for an annulus. Reynolds number, 20,000; r_2/r_1, 3.5.

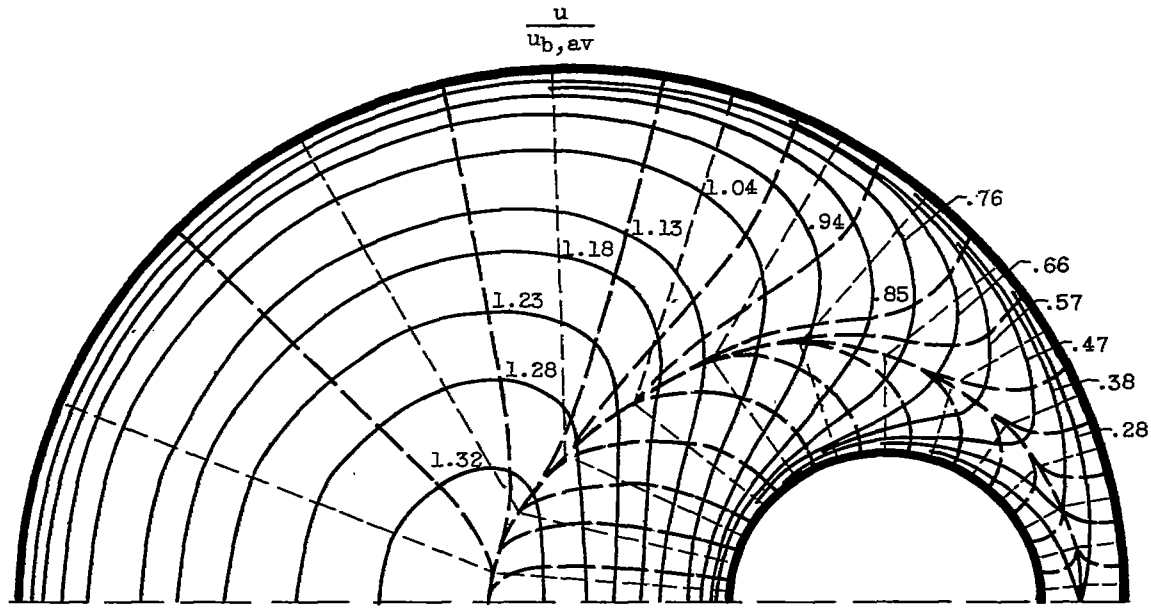

(c) Eccentricity parameter, 0.8.

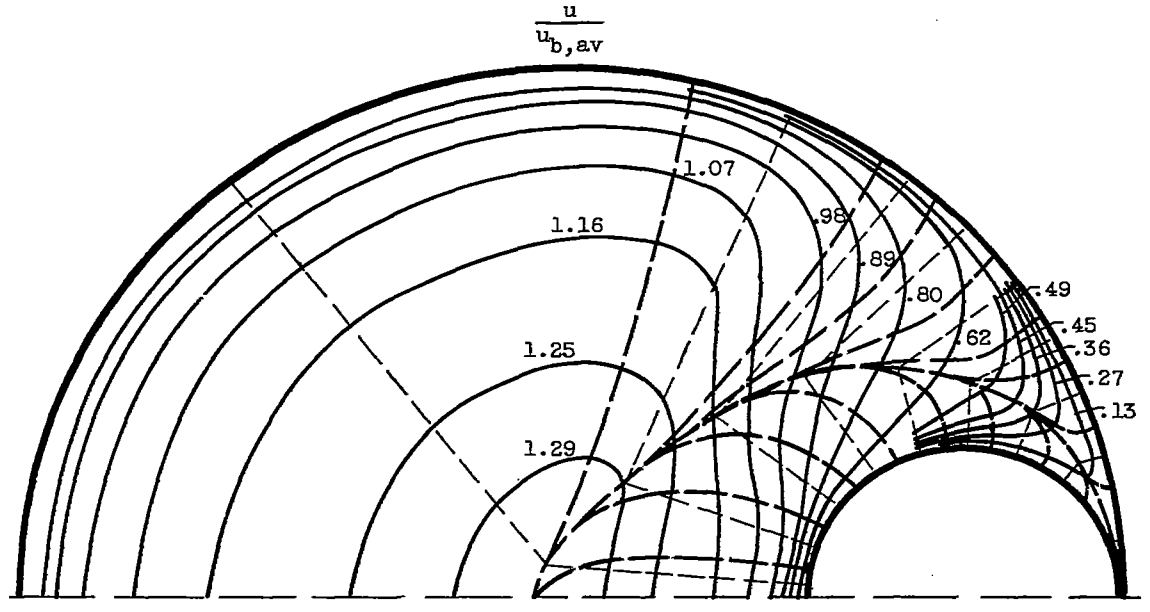

(d) Eccentricity parameter, 1.0.

Figure 3. - Concluded. Predicted velocity distributions for an annulus. Reynolds number, 20,000; r_2/r_1, 3.5.

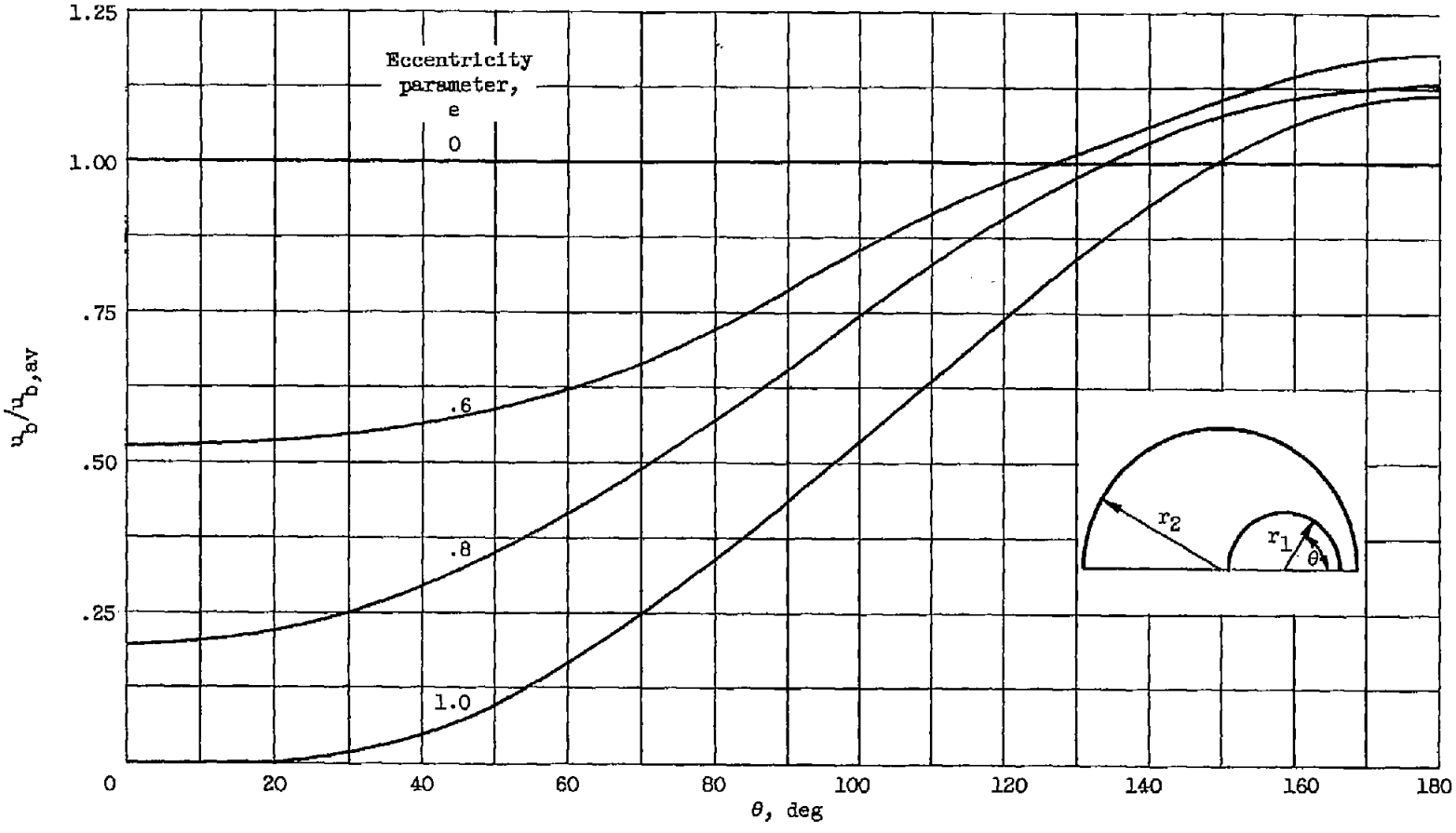

(a) Reynolds number, 20,000.

Figure 4. - Predicted variation of $u_b/u_{b,av}$ with angle θ for various values of eccentricity parameter. r_2/r_1, 3.5.

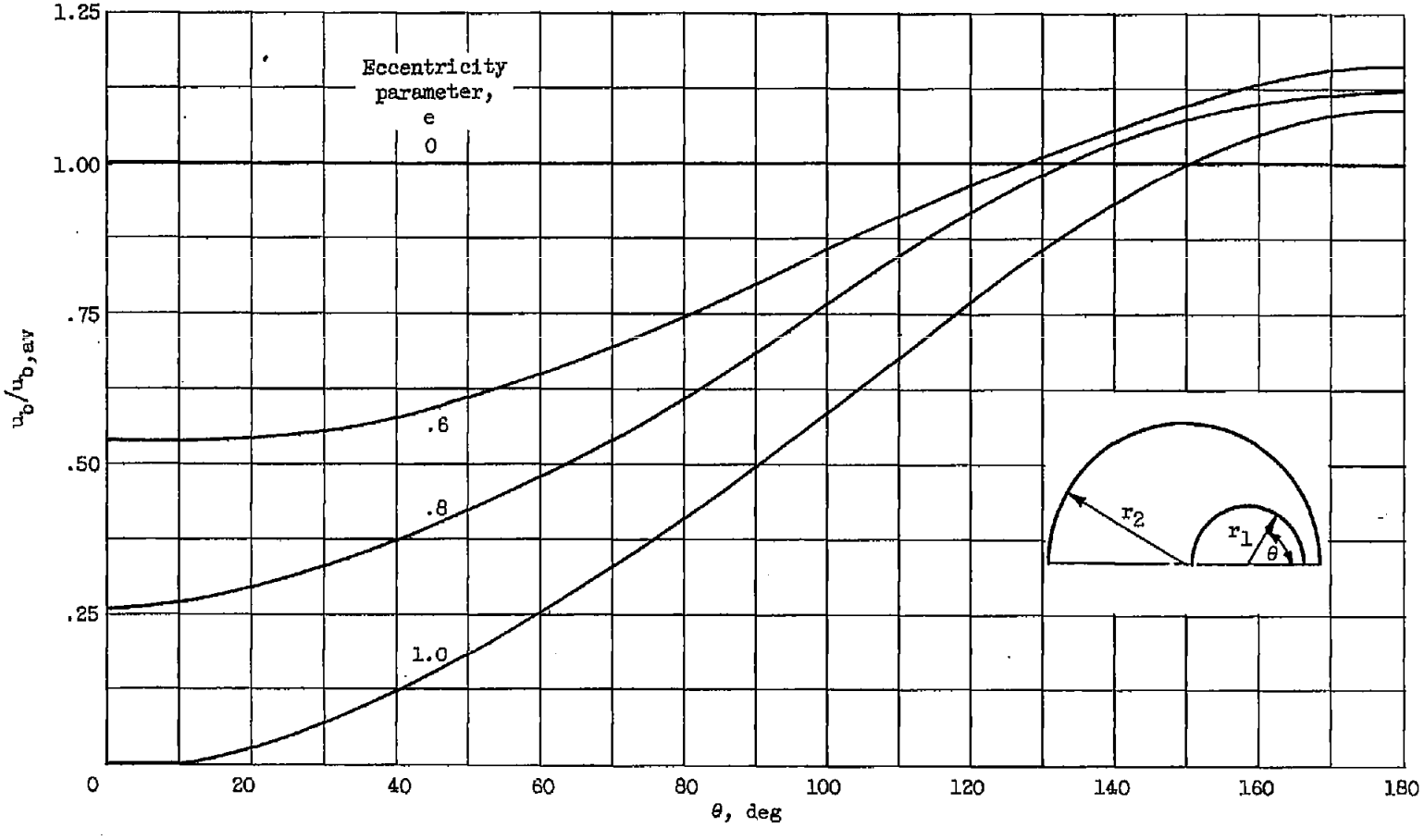

(b) Reynolds number, 600,000.

Figure 4. - Concluded. Predicted variation of $u_b/u_{b,av}$ with angle θ for various values of eccentricity parameter. r_2/r_1, 3.5.

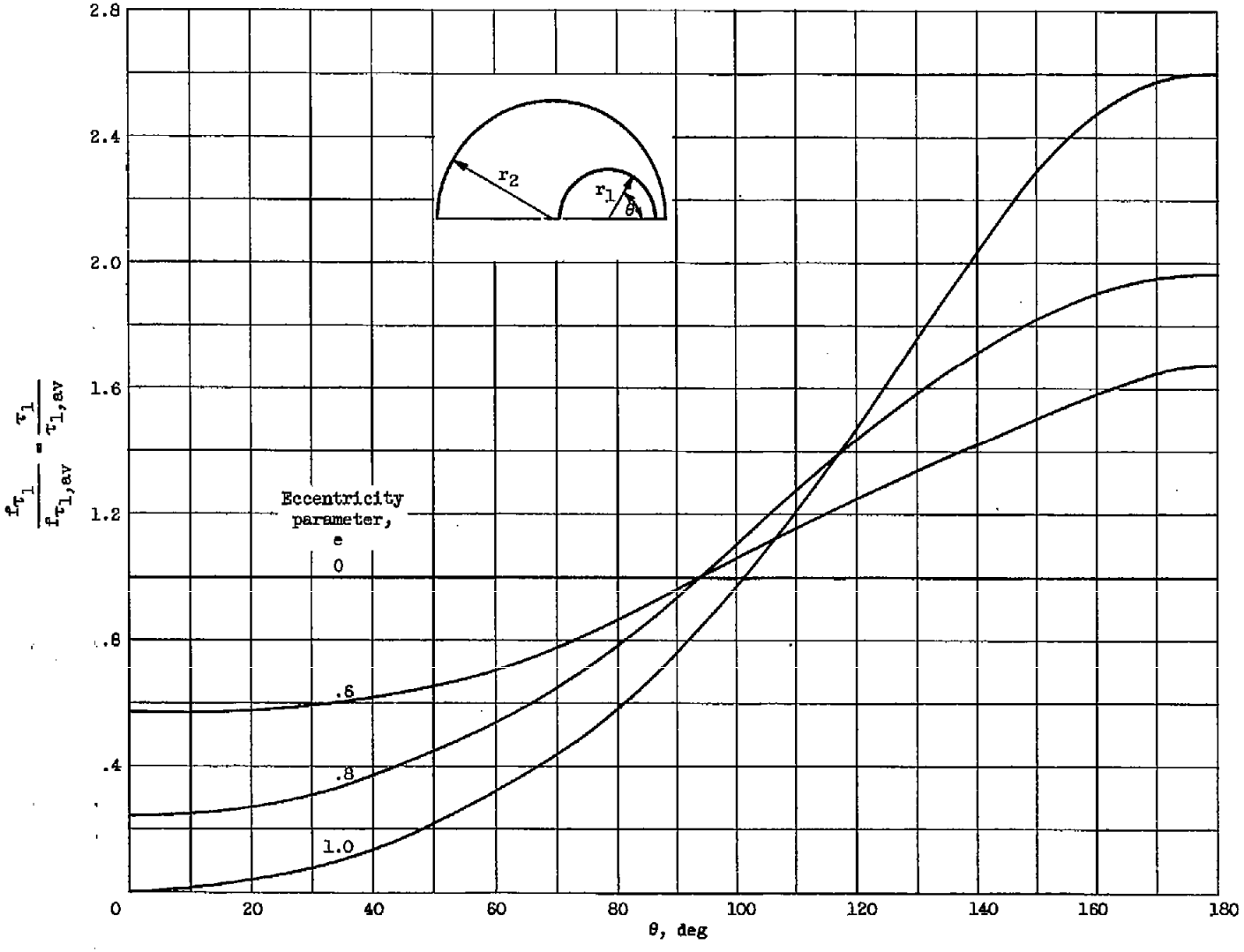

Figure 5. - Predicted variation of shear stress on inner cylinder with angle θ for various values of eccentricity parameter. r_2/r_1, 3.5; Reynolds number, 20,000 and 600,000.

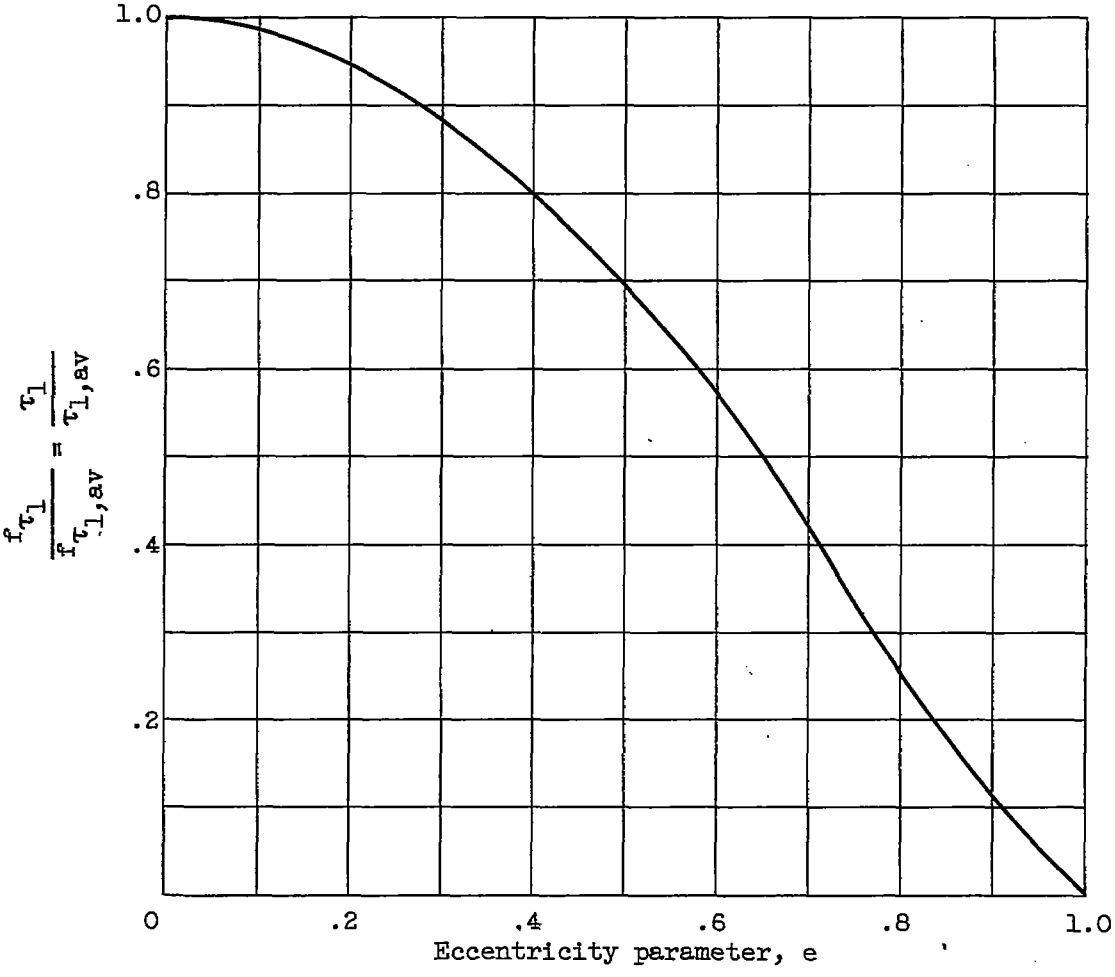

Figure 6. - Predicted variation with eccentricity parameter of shear stress on inner cylinder at point of least separation. r_2/r_1, 3.5; Reynolds number, 20,000 and 600,000.

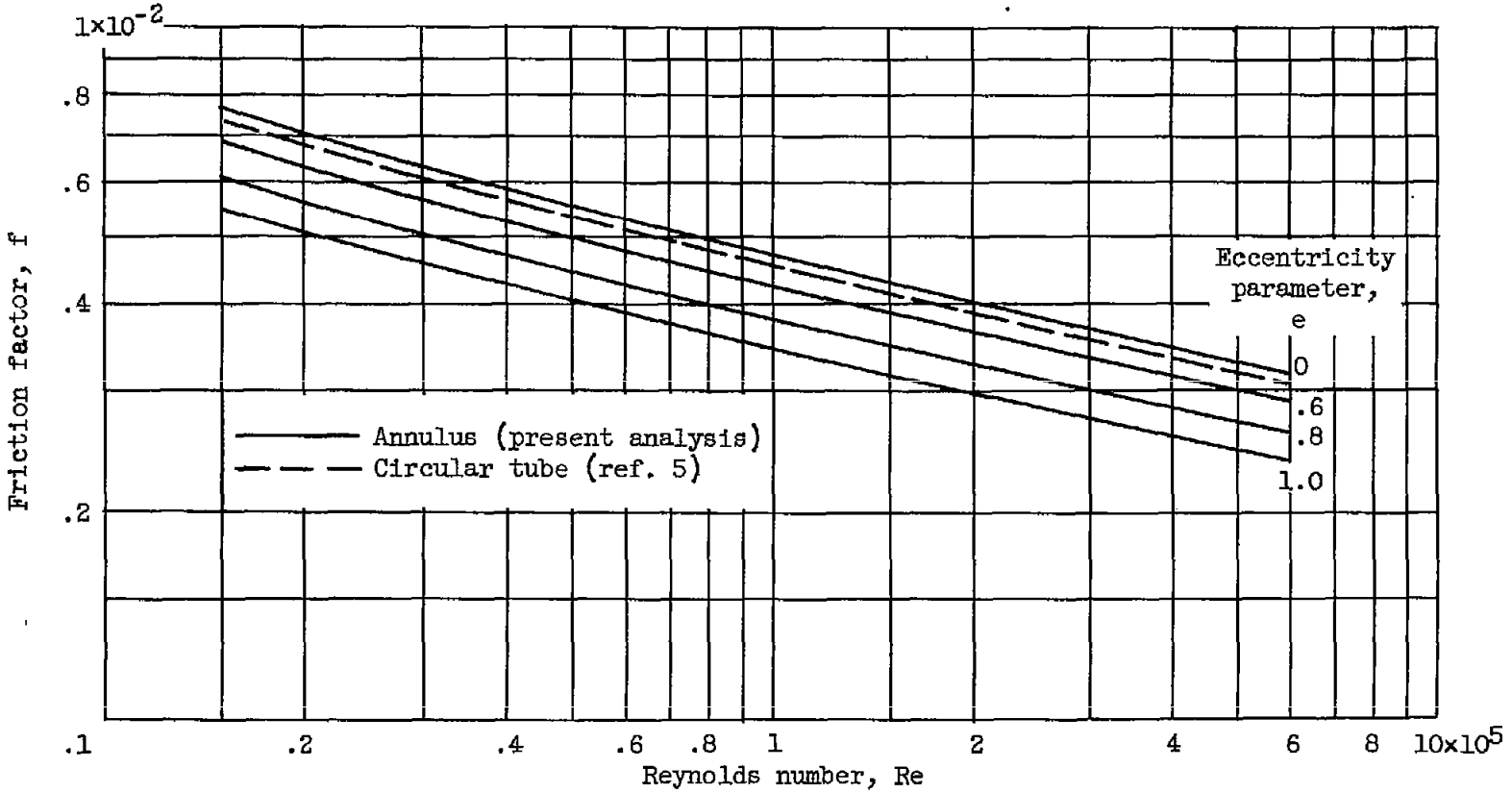

Figure 7. - Predicted variation of friction factor based on static-pressure gradient with Reynolds number and eccentricity parameter. r_2/r_1, 3.5.

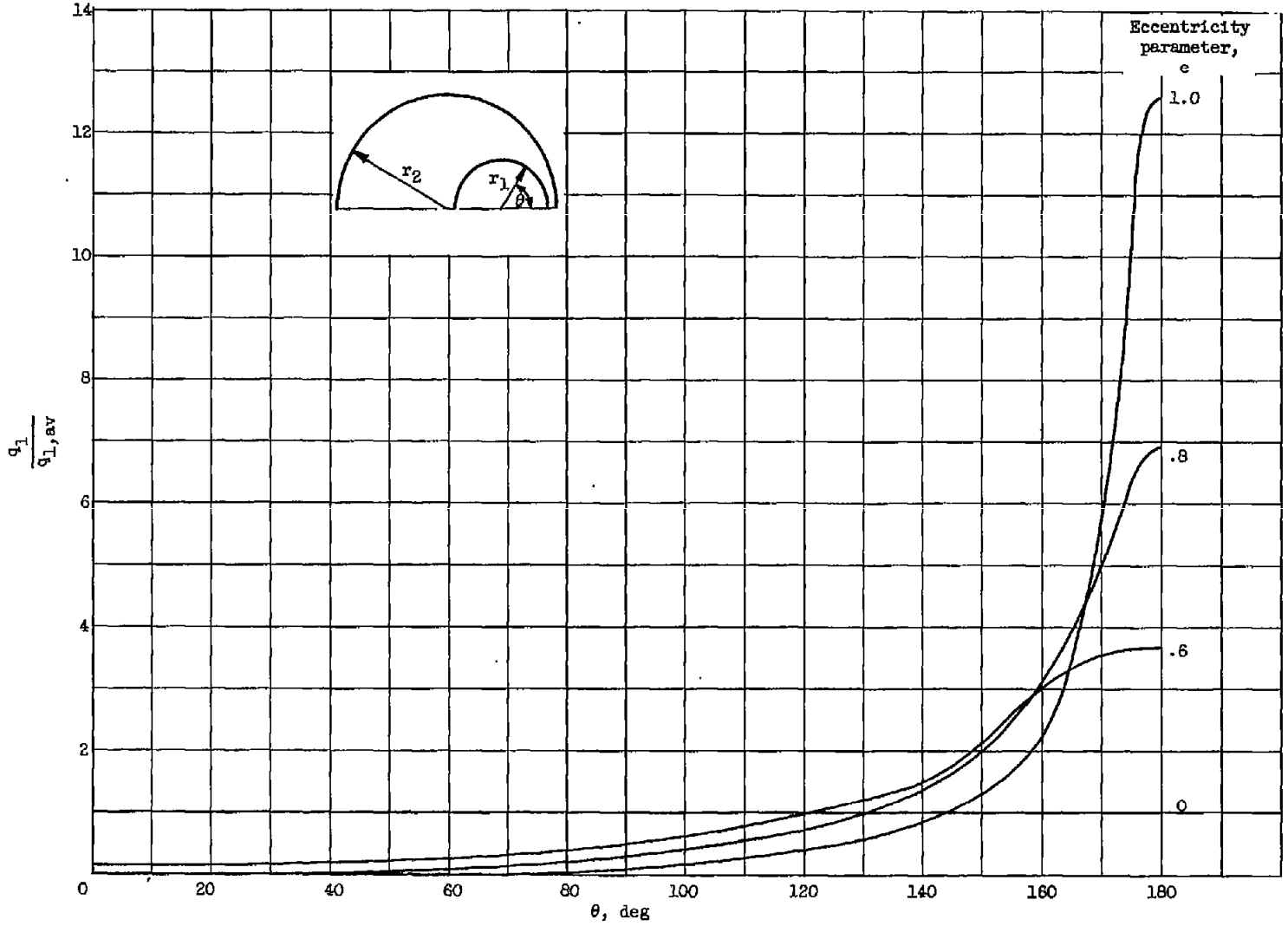

Figure 6. - Predicted variation of heat transfer from inner cylinder with angle θ for various values of eccentricity parameter. r_2/r_1, 3.5; Reynolds number, 20,000 and 600,000. Outer cylinder insulated.

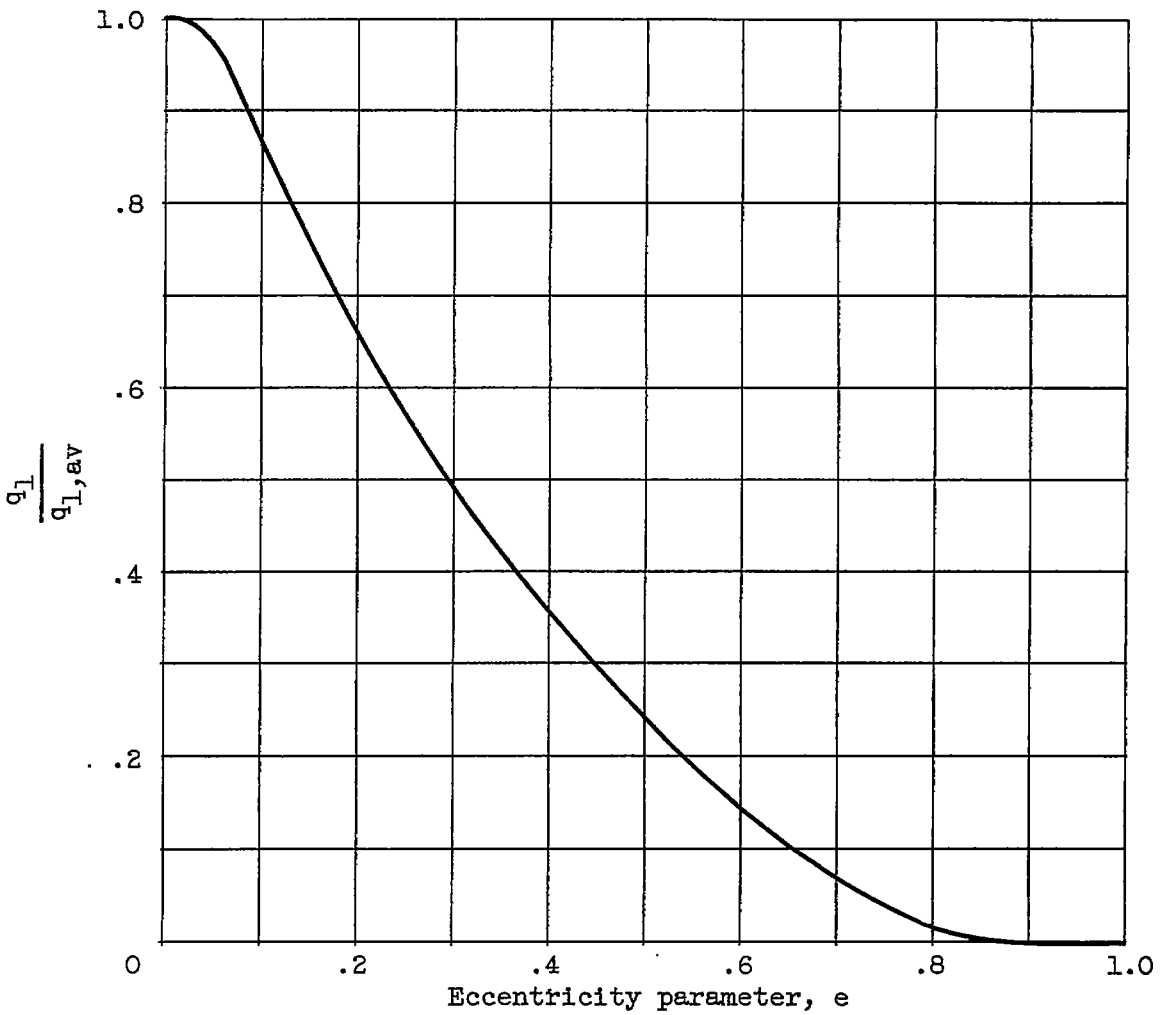

Figure 9. - Predicted variation of heat transfer from inner cylinder at point of least separation with eccentricity parameter. r_2/r_1, 3.5; Reynolds number, 20,000 and 600,000. Outer cylinder insulated.

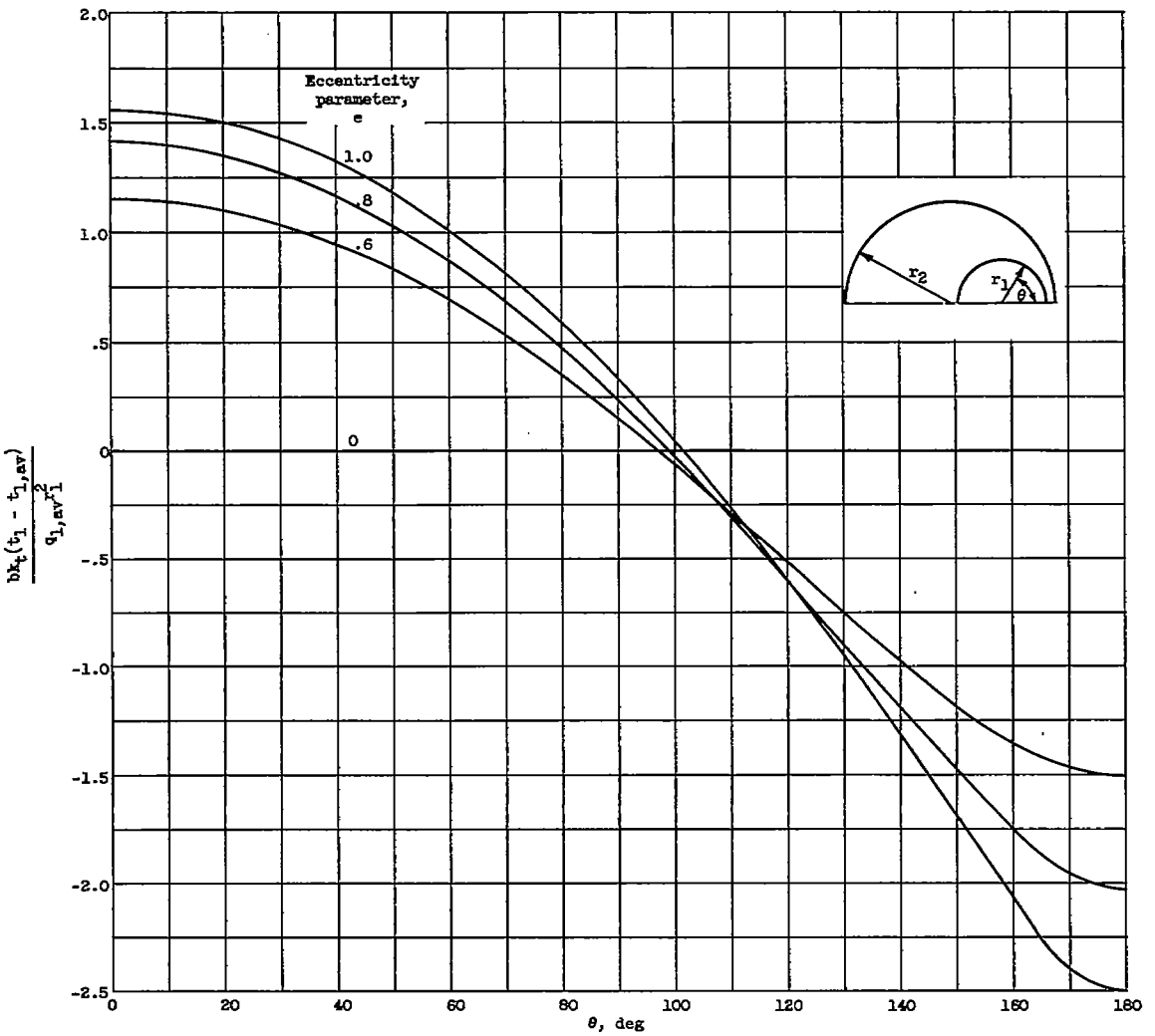

Figure 10. - Predicted variation of wall temperature on inner tube with angle θ for various values of eccentricity parameter. Constant heat flux at inside wall of inner tube; outer cylinder of annulus insulated; r_2/r_1, 3.5; Reynolds number, 20,000 and 600,000.

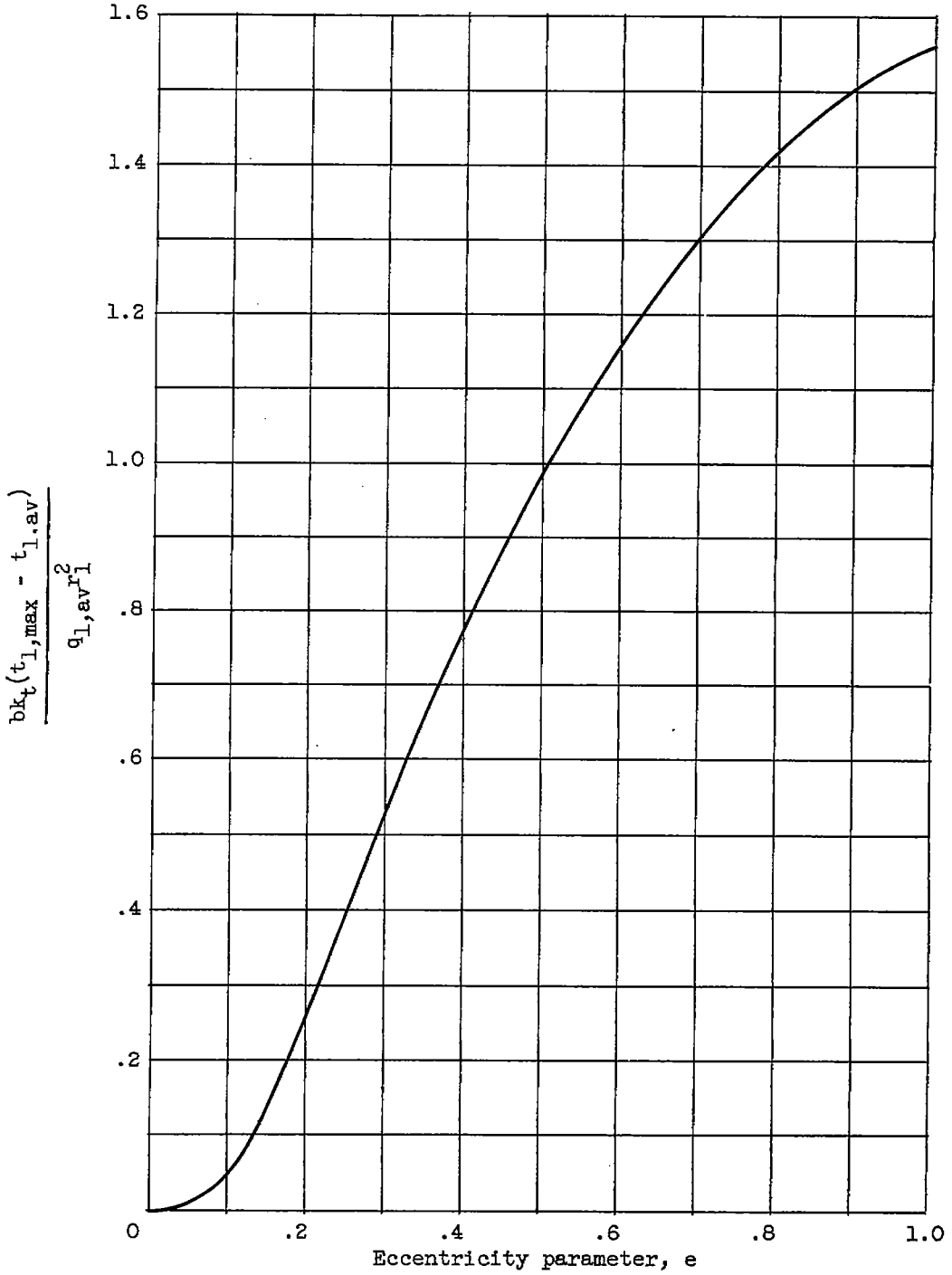

Figure 11. - Predicted variation of maximum temperature difference on inside tube with eccentricity parameter. Constant heat flux at inside wall of inner tube; outer cylinder of annulus insulated; r_2/r_1, 3.5; Reynolds number, 20,000 and 600,000.

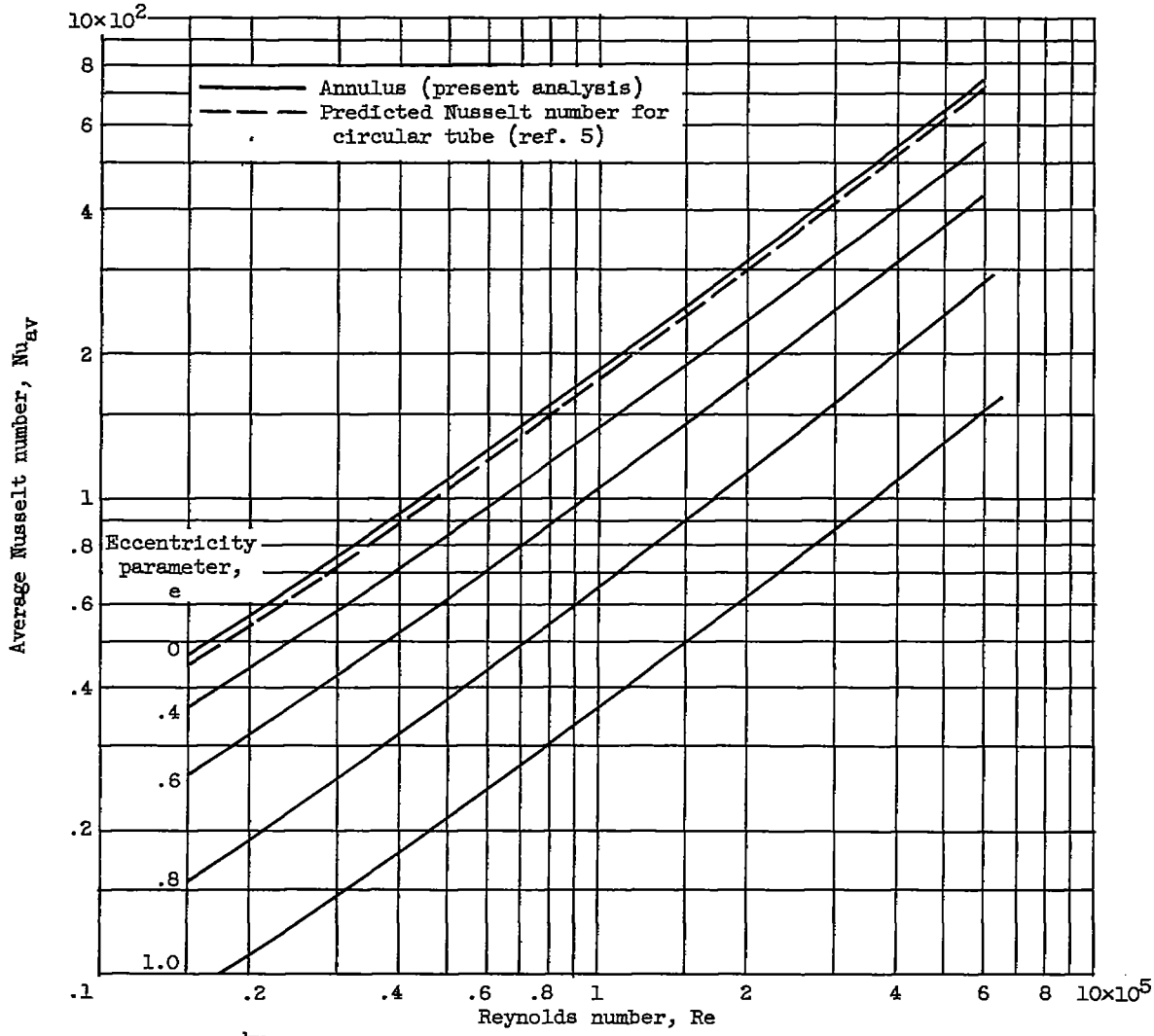

(a) $\frac{kr_1}{k_t b} = 0$ (uniform peripheral wall temperature distribution).

Figure 12. - Predicted variation of average Nusselt number with Reynolds number and eccentricity parameter. Outer cylinder insulated; Prandtl number, 0.73.

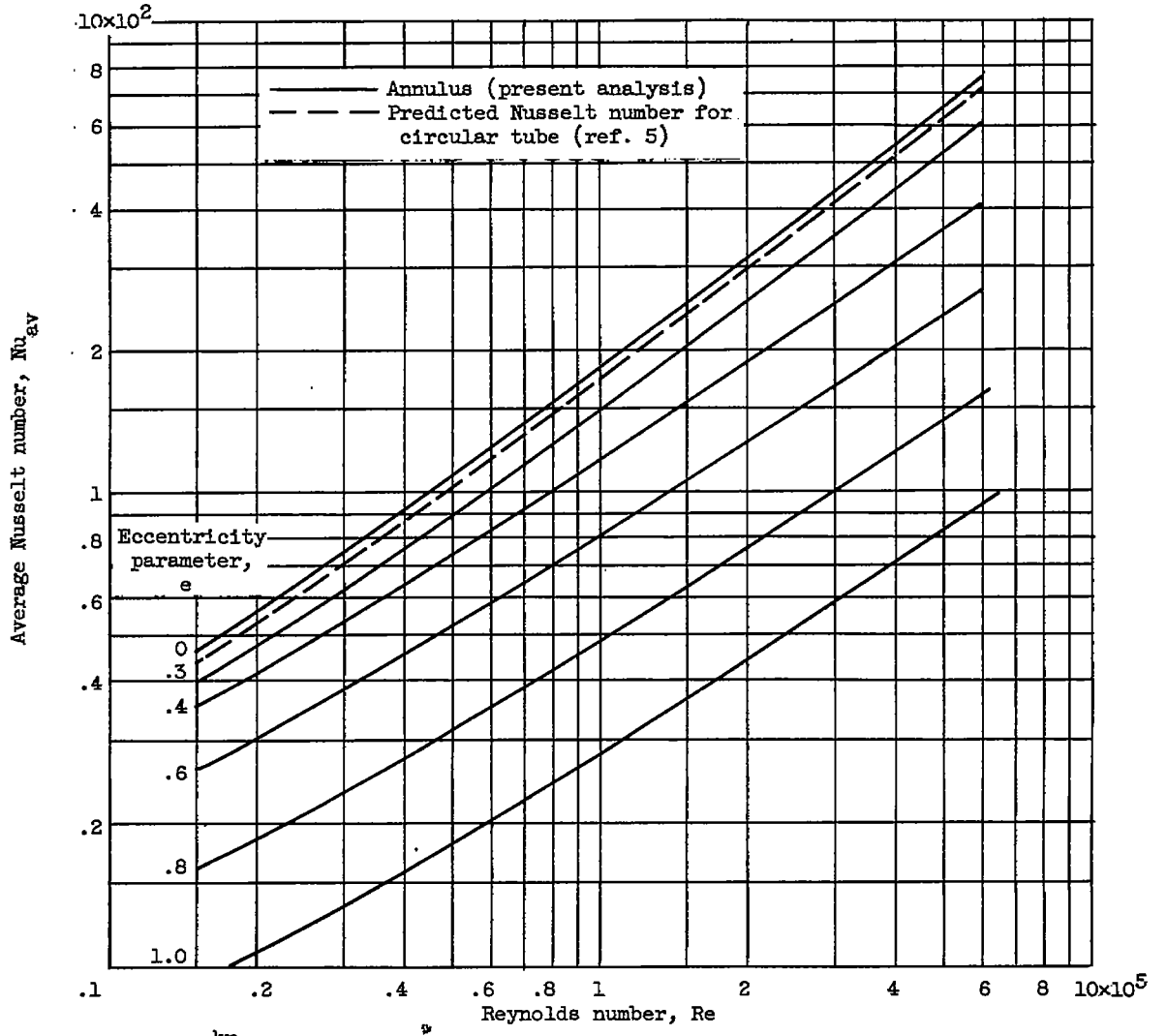

(b) $\frac{kr_1}{k_t b} = 0.01$ (nonuniform peripheral wall temperature distribution).

Figure 12. - Concluded. Predicted variation of average Nusselt number with Reynolds number and eccentricity parameter. Outer cylinder insulated; Prandtl number, 0.73.

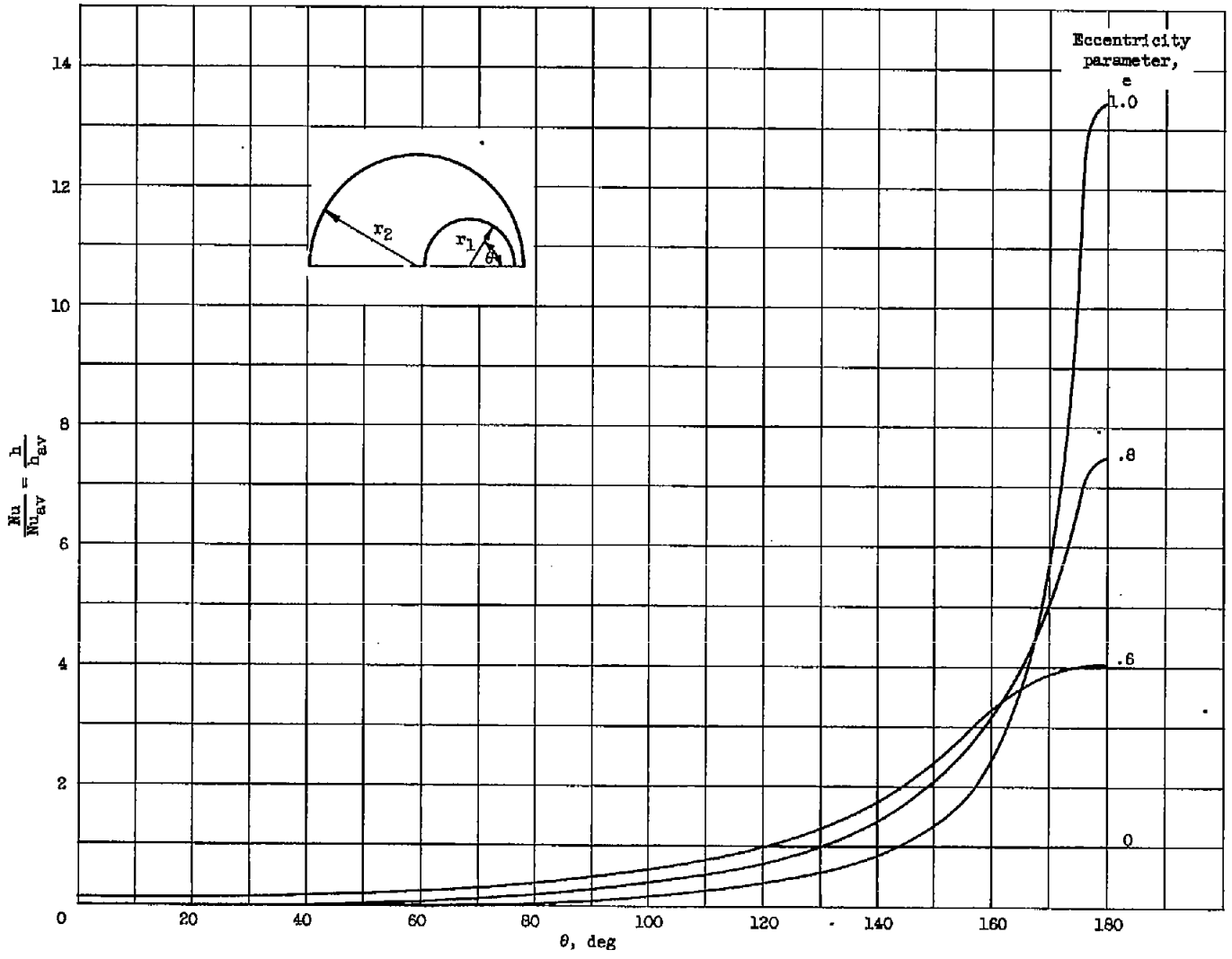

(a) Reynolds number, 20,000.

Figure 13. - Predicted variation of ratio of local heat-transfer coefficient to average heat-transfer coefficient with angle θ for various values of eccentricity parameter. Outer cylinder insulated; r_2/r_1, 3.5; $kr_1/k_t b$, 0.01.

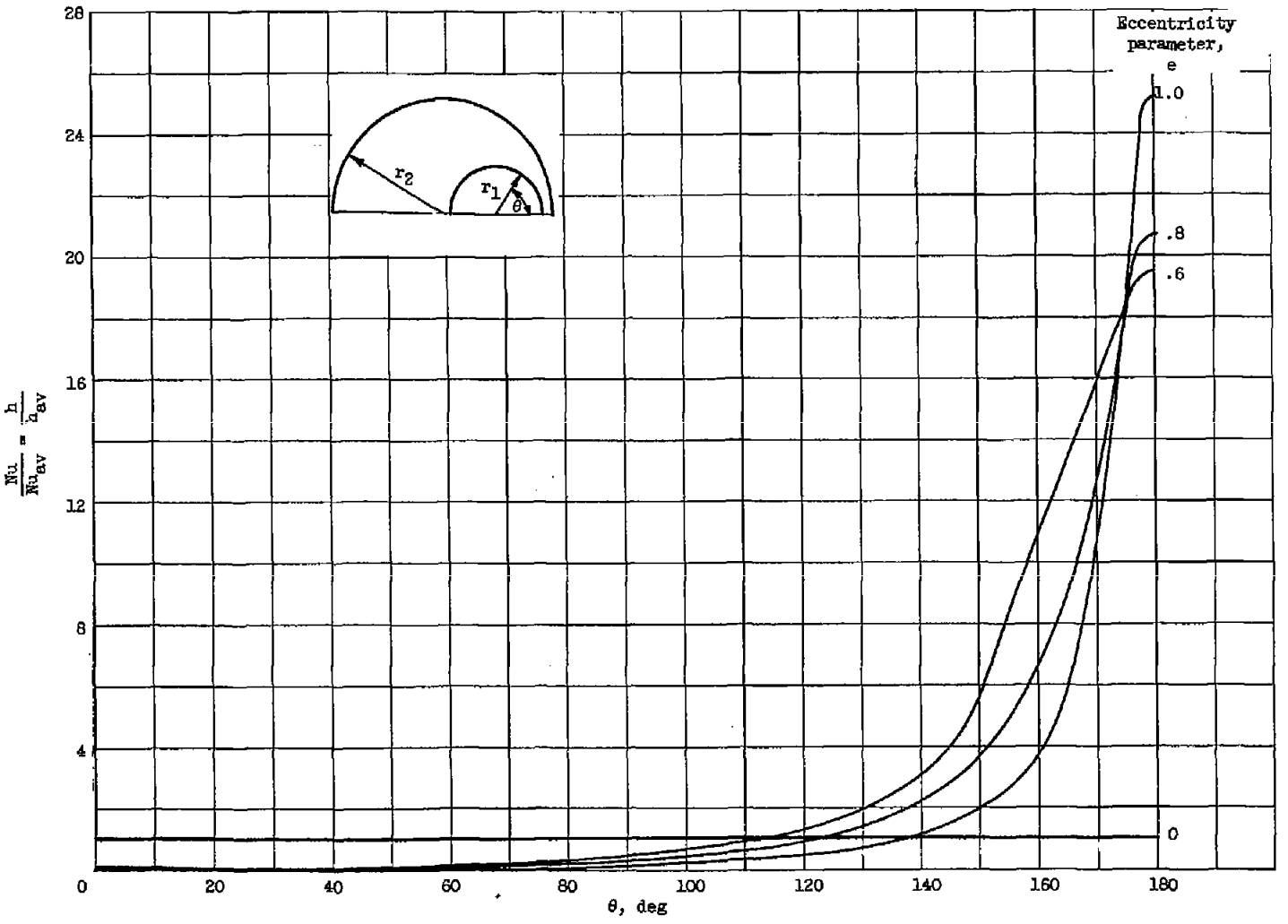

(b) Reynolds number, 600,000.

Figure 13. - Concluded. Predicted variation of ratio of local heat-transfer coefficient to average heat-transfer coefficient with angle θ for various values of eccentricity parameter. Outer cylinder insulated; r_2/r_1, 3.5; $kr_1/k_t b$, 0.01.

NACA - Langley Field, Va.